

QATAR UNIVERSITY

COLLEGE OF ARTS AND SCIENCES

THE APPLICATION OF NANOPARTICLES OF WASTE TIRES IN REMEDIATING

BORON FROM DESALINATED WATER

BY

ELKHATAB ISMAT BABIKER

A Thesis Submitted to the Faculty of

the College of Arts and Sciences

in Partial Fulfillment

of the Requirements

for the Degree of

Masters of Science

in

Environmental Sciences

June 2017

COMMITTEE PAGE

The members of the Committee approve the Thesis of Elkhatab Ismat Babiker  
defended on 22/05/2017.

---

Dr Mohammad Al-Ghouti  
Thesis/Dissertation Supervisor

---

Prof. Gordon McKay  
Committee Member

---

Prof. Nabil Zourai  
Committee Member

---

Dr. Talaat Ahmad  
Committee Member

Approved:

---

Rashid Al-Kuwari, Dean, College of Arts and Sciences

## ABSTRACT

BABIKER, ELKHATAB, Masters : June : 2017, Environmental Sciences

Title: \_The Application of Nanoparticles of Waste Tires in Remediating Boron from Desalinated Water

Supervisor of Thesis: Mohammad Ahmad Al-Ghouti.

A waste tire rubber (WTR) collected from the remains discarded tires has exhibited a noteworthy capacity to adsorb Boron. In the current study, the boron adsorption remediation from water at selected pH values, initial boron concentration, contact time, adsorbent dosage and particle size were examined using the WTR, the chemically modified WTR, and nano-WTR. The adsorption isotherms were best fitted to the Freundlich model with a high correlation coefficient ( $R^2$  :0.89-0.99), while the adsorption kinetics were satisfactorily described by the pseudo second order kinetic equation with correlation coefficient ( $R^2$ : 1).The boron remediation using the WTR, the chemically modified-WTR and nano-WTR at low boron concentration ( $\leq 17.7$  mg/L) were comparable with other adsorbents. The highest adsorption capacities for WTR, chemically modified-WTR and nano-WTR at initial concentration of 17.5 mg/L were  $16.7 \pm 1.3$  mg/g,  $13.8 \pm 1.9$  mg/g and  $12.7 \pm 1.8$ mg/g, respectively.

## DEDICATION

*I dedicate this project to God Almighty my creator, my strong pillar, my source of inspiration,  
wisdom, knowledge and understanding.*

*I also dedicate this work to my Family and close relatives.*

*Finally, I also dedicate this work to my supervisor and supervisory committee members*

## ACKNOWLEDGMENTS

My sincere appreciation goes to my supervisor Dr. Mohammad Al-Ghouti whose contribution and constructive criticism has pushed me to expend the kind of efforts I have exerted to make this work. I also appreciate the efforts and feedback of Prof Nabil Zouari and Prof Gordon McKay throughout the thesis year.

This publication was made possible by UREP # (19-171-1-031) from the Qatar National Research Fund (a member of Qatar Foundation). The findings achieved herein are solely the responsibility of the author(s).

Special thanks also to Dr. Ahmad Elkhatat ( Dept. of Chem. Engineering - Teaching Assistant / Lab Coordinator), Dr. Peter Kasak (CAM- Technical Manager), Mr. Ahmad (CLU- Lab technician), and Mr. Essam Attia (CLU- Senior Chemist) for their effort in assisting in analyzing my samples.

Also special thanks to Office of Graduate Studies and DBES, for their help in providing GA position, which enabled me to learn more and focus on my thesis.

Lastly, thanks to my colleagues and especially Fathy Atia & Ahmad Ahmadi for their support and advice.

## TABLE OF CONTENTS

DEDICATION .....	iv
ACKNOWLEDGMENTS .....	v
LIST OF FIGURES .....	viii
LIST OF TABLES .....	x
<b>Chapter 1: Introduction</b> .....	1
Research Objectives .....	4
<b>Chapter 2: Literature Review</b> .....	5
Overview of Boron Removal Technologies .....	6
Membrane filtration .....	7
Electrodialysis (ED) .....	9
Reverse Osmosis .....	9
Selective Ion Exchange .....	11
Electro-coagulation .....	13
Adsorption .....	14
Toxicity and benefit of boron .....	18
Plants .....	18
Microorganisms .....	18
Animals .....	18
Humans .....	19
Adsorption isotherm .....	19
Isotherm models .....	21
Kinetic studies .....	25
Pseudo first order kinetic model .....	25
Pseudo second order .....	25
Elovich model .....	27
Waste Management of Tire .....	28
Waste Tire as Adsorbent .....	28
Why use chemically modified WTR & Nano-WTR .....	30
Why use FTIR, SEM/EDX and CHN/O to characterize WTR .....	34
<b>Chapter 3: Materials and Methods</b> .....	35
Preparation of Adsorbent .....	35

Preparation of Standard Solutions.....	36
Chemicals.....	36
Preparation of nano-particles from WTR.....	36
Preparation of chemically treated WTR and nano-WTR.....	36
Characterization of the adsorbents.....	37
Fourier Transform Infrared (FTIR).....	37
Scanning electron microscope (SEM)/EDX.....	37
CHN/O elemental analyzer.....	37
Experimental Procedure – Batch Adsorption test and Isotherm study.....	37
Batch Adsorption.....	37
Analysis of Samples.....	38
Parameters of the study.....	38
Experimental Procedure – kinetic studies.....	39
WTR Leachability test.....	39
Statistical Design of Experiments.....	40
<b>Chapter 4: RESULTS AND DISCUSSION.....</b>	<b>41</b>
Characteristics of WTR, nano-WTR and its modified forms.....	41
FTIR characterization.....	41
Boron adsorption by WTR.....	47
pH effect on Boron adsorption by WTR.....	47
Adsorbent dosage effect on Boron adsorption by WTR.....	48
Adsorbent particle size effect on Boron adsorption.....	50
Initial Concentration effect on the adsorption of Boron on WTR.....	51
Boron adsorption by chemically modified WTR.....	53
pH effect on Boron adsorption by chemically modified WTR.....	53
Initial Concentration effect on Boron adsorption by chemically modified WTR.....	54
Boron adsorption by Nano-WTR.....	55
Initial Concentration effect on Boron adsorption by Nano-WTR.....	55
Leachability of WTR.....	55
Isotherm Models.....	57
Langmuir and Freundlich Adsorption Isotherm.....	57
Kinetics of adsorption.....	62
<b>Chapter 5: Conclusion.....</b>	<b>72</b>
References.....	74

## LIST OF FIGURES

<i>Figure 1: Boron Speciation with a total boron concentration of <math>c_{B, total} = 0.7 M</math> (Schott et al., 2014).....</i>	7
<i>Figure 2: Filtration spectrum of membrane technology (Mazille &amp; Spuhler, 2012).....</i>	8
<i>Figure 3: The scheme of ED separation of ionic species. Source: (Strathmann, 2004) .....</i>	9
<i>Figure 4: Reverse Osmosis process diagram. Source: (Güler et al., 2015). .....</i>	10
<i>Figure 5: Types of Ion exchange resins (ASTOM, 2013). .....</i>	12
<i>Figure 6: Types of Ion exchange membranes (ASTOM, 2013).....</i>	13
<i>Figure 7: Electrocoagulation Process (WaterTectonics, 2017). .....</i>	14
<i>Figure 8 Fundamentals of adsorption and desorption process on the adsorbent .Source: (Henning &amp; Degel, 1990).....</i>	17
<i>Figure 9: Adsorption Isotherm. Source:(Amrita institute of education, 2012).....</i>	20
<i>Figure 10: Classification of adsorption isotherms (Amrita institute of education, 2012). I: Micro porous Materials; II: Non porous Materials; III: Non porous materials and materials which have the weak interaction between the adsorbate and adsorbent; IV: Mesoporous materials; V: Porous materials and materials that have the weak interaction between the adsorbate and adsorbent and VI: Homogeneous surface materials.....</i>	21
<i>Figure 11: Reactions for preparation of the modified ground tire rubber; halogenation of carbon-carbon double bond, Aminolysis of halogenated ground tire rubber, followed by treatment by HCl to yield ETD modified ground tire rubber. Source : (Rungrodnimitchai &amp; Kotatha, 2015b).....</i>	31
<i>Figure 12 Reactions for preparation of the modified WTR ;(1) Bromination of carbon-carbon double bond, (2) Aminolysis of dibromide product, and (3) Protonation of Ethylenediamine modified WTR. Source : (Rungrodnimitchai &amp; Kotatha, 2015b).....</i>	32
<i>Figure 13 Preparation of Adsorbent, whereas a: cutting tire by hacksaw; cutting by knife, etc.; c-f: shredding &amp; grinding to micro-size; g: dry at oven after cleaning; and h: sieving WTR .....</i>	35
<i>Figure 14: The FTIR spectra for WTR &amp; Chemically modified WTR .....</i>	41
<i>Figure 15: SEM micrograph of (a) WTR ,(b) NanoWTR ,(c) <math>HNO_3</math> 1:3 <math>H_2SO_4</math> ,(d) <math>H_2SO_4</math> (e) <math>HNO_3</math> 1:1 <math>H_2SO_4</math> ,(f) <math>HNO_3</math> ,(g) <math>HNO_3</math> 3:1 <math>H_2SO_4</math> .....</i>	43
<i>Figure 16: EDX Elemental Analysis of (a) WTR, (b) NanoWTR, (c) <math>HNO_3</math> 1:3 <math>H_2SO_4</math> ,(d) <math>H_2SO_4</math> (e) <math>HNO_3</math> 1:1 <math>H_2SO_4</math> ,(f) <math>HNO_3</math> ,(g) <math>HNO_3</math> 3:1 <math>H_2SO_4</math> .....</i>	46



Figure 17: pH Effect on the adsorption of Boron on WTR.....	48
Figure 18: Dosage of adsorbent effect on Boron adsorption. ....	49
Figure 19: Particle size effect on boron adsorption. ....	51
Figure 20: Initial Concentration effect on the adsorption of Boron on WTR.....	52
Figure 21: pH effect on the adsorption of Boron on chemically modified WTR. Where ratio 1: HNO <sub>3</sub> , ratio 2:H <sub>2</sub> SO <sub>4</sub> , ratio 3: HNO <sub>3</sub> 3:1 H <sub>2</sub> SO <sub>4</sub> , ratio 4: HNO <sub>3</sub> 1:3 H <sub>2</sub> SO <sub>4</sub> and ratio 5: HNO <sub>3</sub> 1:1 H <sub>2</sub> SO <sub>4</sub> ; And Where pH class 1: pH 2 , pH class 2: pH 4, pH class 3: pH 6, pH class 4: pH 7, pH class 5: pH 8, pH class 6: pH 10, pH class 7: pH 12.....	53
Figure 22: Initial concentration effect on the boron adsorption on chemically modified WTR .....	54
Figure 23: Initial Concentration effect on the adsorption of Boron on Nano-WTR.....	55
Figure 24: Heavy Metals Leachability from WTR.....	56
Figure 25: Linearized Langmuir Adsorption Isotherms plotted for batch adsorption experiment, Where A: WTR, B: Nano-WTR and C: Chemically Modified WTR. ....	59
Figure 26: Freundlich Adsorption Isotherms plotted for batch adsorption experiment, Where A: WTR, B: Nano-WTR and C: Chemically Modified WTR.....	60
Figure 27: Boron removal percentage as function of time for 2 WTR dosage (1g and 1.5 g).....	63
Figure 28 Lagergren Pseudo first order kinetic model plotted for adsorption study of WTR; where A: for 1.5g WTR, B: 1 g WTR ; Operational settings: Adsorbate mass : 1 g, Solution volume :1700 ml, Contact time : minutes, Temperature : 294.45 K , Rotation speed: 150 rpm , pH : 2.....	64
Figure 29 Pseudo second order kinetic model plotted for adsorption study of WTR; where A: for 1.5g WTR, B: 1 g WTR, and 1-4: Pseudo-second order Linearized version number.....	66
Figure 30 Elovich kinetic model fitted for adsorption study of WTR; where A: for 1.5g WTR, B: 1 g WTR ; Operational settings: Adsorbate mass : 1 g, Solution volume :1700 ml, Contact time : minutes, Temperature : 294.45 K , Rotation speed: 150 rpm , pH : 2.....	69

## LIST OF TABLES

<i>Table 1 Differences Between Physical &amp; Chemical Adsorptions</i> .....	15
<i>Table 2 Removal Efficiency And Evaluation Of Various Technologies For Boron Removal</i> .....	17
<i>Table 3: R<sub>L</sub> Values And Type Of Isotherm (Aisien Et Al., 2013; Karthikeyan and Siva Ilango, 2008).</i> .....	23
<i>Table 4: Pseudo Second -Order Kinetic Be Linearized Versions</i> .....	26
<i>Table 5: Analysis Of Waste Tire Rubber (Aisien et al., 2013).</i> .....	29
<i>Table 6: Ultimate Elemental Analysis Of Waste Tire Rubber(Aisien Et Al., 2013).</i> .....	29
<i>Table 7 Results of published citations on application of WTR as adsorbent</i> .....	33
<i>Table 8 Most Significant Bands Of WTR(Colom Et Al. 2016).</i> .....	42
<i>Table 9: EDX Elemental Analysis -Wt.(%) of Element</i> .....	45
<i>Table 10: Characteristics Of WTR Compared To Other Studies</i> .....	47
<i>Table 11 Parameters For Langmuir And Freundlich Isotherms</i> .....	60
<i>Table 12 Comparison Of This Study With Other On Freundlich Isotherm On The Use Of WTR As Adsorbent</i> ..	61
<i>Table 13 Parameter Values For Pseudo First Order, Pseudo Second Order and Elovich Models</i> .....	67
<i>Table 14: Adsorption Isotherms Of Boron For Various Adsorbents (Morisada Et Al., 2011)</i> .....	71

## **Chapter 1: Introduction**

In the Gulf, there has been a lack of large freshwater mainly due to the lack of annual rainfall along with geological characteristics. The population growth rate in Qatar has increased dramatically, particularly over the past five years. Therefore, desalination units has been extensively used in these areas to get clean water for drinking and irrigation. However, with host the 2022 World Cup in Qatar and to cope with the influx of hundreds of thousands of visitors, the country need adequate water and sewage infrastructure. Ras Abu Fintas water plant provides 50% of the water needs of the State of Qatar. Qatar has thermal desalination stronghold over the years. However, this has been changed recently as Qatar has granted the first large scale RO contract to develop the Ras Abu Fintas A3 project. It is the first large-scale, reverse osmosis (RO) desalination plant in the country. And the work has been started in the third quarter of 2016, according to a report published in a local newspaper (MDPS, 2015).

The water that comes from desalination water units may contain a high boron concentration. Generally, at this circumstance, boron adsorbs in soils as it will not be satisfactorily leached by rain and; therefore accelerating boron deposition in plants and soils. Accordingly, a low water boron concentration from desalination plants would highly be favorable. For certain metabolic activities, a very low concentration of boron would be needed, but with a higher boron concentration, plant growth will be affected; exhibiting yellowish spots on leaves and fruit. 0.3 mg/L boron would be acceptable in the irrigation water for some plants. In addition, high boron concentration in drinking water can cause male reproductive barriers (Redondo Busch & De Witte, 2003).

As there is an increase in the need for fresh water throughout the world, there is a necessity to implement innovative methodologies that would deal with non-conventional water sources. In seawater, typical boron concentration can be reached to 7 mg/L and in the range of 4.5– 5.0 mg/L in the Arabian Gulf. EU recommends maximum boron concentration in drinking water as 1.0 mg/L and WHO sets a limit of 0.3 mg/L for drinking water boron but recently in 2011, this value has been revised as 2.4 mg/L.

Thermal desalination technology is the effective technology in removing seawater boron to nearly zero concentration. This efficiency in removing boron is not emulated by RO desalination technology where elimination of boron is revealed to be inadequate. It could be attributed to the large quantity of seawater boron normally exists as  $B(OH)_3$  which can easily pass through the RO membrane. Therefore, boron elimination from water is highly required for RO desalination units. Currently, owing to increasing request of safe drinking and irrigation water, RO desalination has become more favorable, dominant and potential method than thermal desalination. According to our preliminarily studies, the concentration of Boron in the collected waters is the range of 0.4-0.6 mg/L (Prats et al., 2000).

Prats et al., (2000) showed that at pH ranges of 5.5–9.5, the rejection of  $B(OH)_3$  was reached to 40–60% while  $B(OH)_4^-$  removal was about 95%. Thus, the boron elimination by RO is reliant on the  $B(OH)_3/B(OH)_4^-$  ratio. With a high percentage of  $B(OH)_3$  in the feeding water will cause unacceptable levels of boron in the treated water. However, the existing RO membrane for boron treatment has the capability to treat boron for 85 to 90% which represents around 80% boron rejection at (pH 8, 55.2 bar, 25°C). With the purpose of boron reduction in RO permeate and following the rigorous requirements, numerous technical designs and concepts have been developed from the technical & economical aspect. However, the cost for typical water production is 0.38–0.50 \$/m<sup>3</sup> for 0.6–1 mg/L boron. Furthermore, the boron removal by RO is influenced by many causes, for instance, initial boron

concentration, pH, temperature, flow rate, pressure and others. Therefore, it would be critical to observe a relationship between the boron removal percentage and the above-mentioned parameters.

Waste management is an important topic. The quantity of waste is considerably rising for many years all over the world. The tires disposal shows a key environmental concern in many countries. Consequently, the management of waste tire Rubber (WTR) has turn out to be a great concern. Therefore, finding new methods to reuse the WT is of importance (Kim et al.,1997).

There are several method of waste tire disposal such as landfill, energy recovery, and reutilization in sports surfaces and roofing materials. However, most of the countries firmly bans the disposal of waste tire on landfill and use them as a fuel because of the environmental problems that may arise owing to the emission of hazardous pollutants. The waste tire structure contains double bonds which are useful for chemical modification. It is derived from isoprene units of natural rubber and butadiene polymer units of synthetic rubber (Rungronmitchai & Kotatha, 2015a).

There are several wastewater treatment technologies such as the application of adsorbents' usage for water remediation is broadly studied. For instance, biosorbents presented outstanding metals adsorption. Lately, nano-adsorbents were described as practical materials. Activated carbon is an excellent adsorbent for wastewater remediation. Several types of activated carbon from WTR were studied for metals and organic pollutants removal by several authors. However, some authors studied the adsorbents preparation from chemical treatment of WTR. For an example, Vizuite et al. 2004 studied the modification of WTR by heating at 400°C and chemical modification by H<sub>2</sub>SO<sub>4</sub> and HNO<sub>3</sub> to enhance the Hg<sup>2+</sup> adsorption. Katyaem et al. 2006 investigated the phenol elimination of wastewater using

nanoparticles of WTR. It was concluded that smaller particles presented excellent enhancement for the phenol adsorption (Rungronmitchai & Kotatha, 2015b).

According to National Nanotechnology Initiative- USA (NNI), Nanoparticles are a remarkable material with excellent properties to add the structure of adsorbent material. Certainly, nanoparticles increases the adsorption efficiency and capacity, alter in kinetics and thermodynamics of adsorption. This study also focused on producing nanoparticles from WTR to explore the changes in adsorption properties for boron remediation from aqueous media. It is already known that particles size is a significant factor determining the rate of adsorption. It is identified that nanoparticles quickly and completely adsorbed pollutants from wastewater. As a particle turn into smaller ones, its surface area becomes much higher; enhancing their adsorption efficiency and capacity.

#### Research Objectives

The objective of this research were to (a) develop an economical and environmentally acceptable remediation methods using nano-WTR, (b) evaluate the process with respect to selectivity and efficiency, and (c) produce chemically modified WTR for high boron remediation. In order to achieve the above objectives, several tasks were carried out: (1) Examining the physical and chemical characterizations of the WTR; (2) Preparing nanoparticles and chemically modified forms from WTR; (3) Examining the boron remediation characteristics using WTR, nano-WTR and its chemically modified forms; (4) Characterizing the adsorbents using various analytical techniques such as Fourier transform infrared (FTIR), SEM/EDX, and CHN/O Analysis; (5) Leachability test for the WT and; (6) Statistical analysis.

## Chapter 2: Literature Review

Boron is discharged into the environment from several sources such as agriculture, industrial effluents and enameling processes and from the natural leaching of minerals. Boron compounds are found in seawater resulting in boron salts in coproduced waters from the oil and gas exploration and recovery operations (Redondo et al., 2003). The forms of boron salts include borax, boric acid and mineral borates and several complex forms, however, at the concentrations in the order of 5-6 mg/L. Boron also exists in its mononuclear forms: boric acid,  $B(OH)_3$  and  $B(OH)_4^-$ . High levels of boron are toxic to human and plant, and can cause severe health problems. The World Health Organization has set a recommended level of boron in drinking water to be below 2.4 mg/L (Parks & Edwards, 2005).

In the Middle Eastern countries, there is a severe lack of fresh drinking water and in Qatar almost all the drinking water comes from the desalination of seawater. Currently, the desalination plants in Qatar are thermal based, and consequently the water produced is low in boron; but there is an increasing demand for more drinking and agricultural water and it has been proposed to construct the first large scale reverse osmosis, RO, desalination plant in Qatar commencing in late 2016. The effectiveness for boron removal is not as pronounced for RO desalination plants as it is with thermal desalination plants and this produced water may contain boron. To avoid environmental complications of high level of boron in water, boron remediation is required by an appropriate method.

Boron is acknowledged as a vital micronutrient vegetation and animals with thin range between its deficiency and excess. The boron abundance in the environment supposedly triggers the endemic symptoms and diseases among humans and cattle (Parks & Edwards, 2005). It is a vital vegetation nutrient, required mainly for sustaining the function of wall of cells. Nonetheless, high soil concentrations greater than 1.0 mg/g leads to tip necrosis in leaves and poor growth performance. Approximately all vegetation, including boron

tolerant vegetation, will express signs of boron toxicity when soil boron content is bigger than 1.8 mg/g. If boron concentration goes beyond 2.0 mg/g, a small number of vegetation will functions well and the rest will not survive. If boron concentrations in plant tissue go beyond 200 mg/g, signs of boron toxicity are expected to manifest. Nonetheless, vegetation vary in their tolerance to surplus boron. For example, vegetation such as beans and peas are exceptionally sensitive, whereas alfalfa is moderately tolerant to high boron concentrations. Consequently, boron should be added to the soil at low rates only after a proven need has been recognized through vegetation tissue and/or soil testing (Parks & Edwards, 2005; Blevins & Lukaszewski, 1998).

## Overview of Boron Removal Technologies

There is no simple and effective method for remediating  $B(OH)_3$  and borate,  $B(OH)_4^-$  from water. In literature, it is shown that coagulation, sedimentation, and filtration do not considerably remediate boron; and therefore special treatment methodologies are required to eliminate high boron concentration. Moreover, other treatment methods such as ion exchange and RO would considerably remove boron from water but are probably to be extremely expensive.

In aqueous media, several species of dissolved boron is present; depending on several factors such as concentration and pH in water, in phenomena which is known boron speciation. Boron speciation acts when a total boron concentration higher than 25 mmol/L, and it forms polyborates (tri-, tetra- and pentaborates) in the pH range from 4 to 13. (Schott et al., 2014). A speciation boron diagram is shown in Figure1 for the pH range 0 to 14.



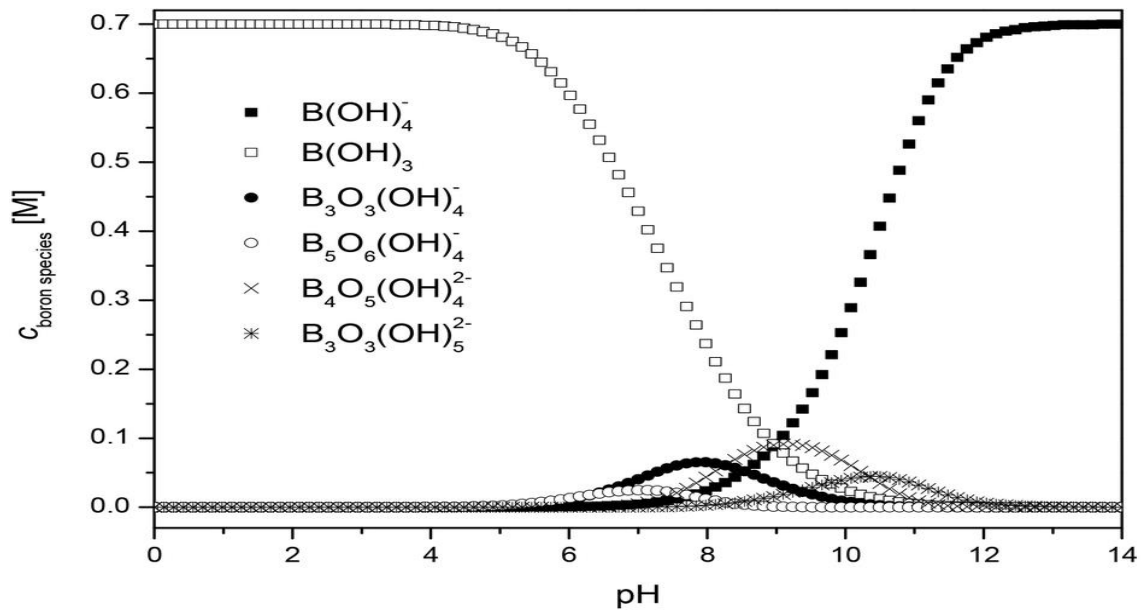


Figure 1: Boron Speciation with a total boron concentration of  $c_{B, \text{ total}} = 0.7 \text{ M}$  (Schott et al., 2014).

In summary, at low concentration ( $\leq 216 \text{ mg/L}$ ), boron primarily exists as boric acid,  $B(OH)_3$  and borate,  $B(OH)_4^-$ . At higher boron concentration and a high pH value, polynuclear boron species would be formed such as  $B_2O(OH)_6^{2-}$  or  $B_5O_6(OH)_4^-$ . Therefore, as boron concentration in seawater is in the range of 4.5– 5.0 mg/L, it would be satisfactory that only mononuclear boron species are present in seawater.

### Membrane filtration

In the 1960s, through the advance of high efficacy synthetic membranes, membrane filters emerged as a worthwhile technology of water purification. Application of membranes for water treatment has developed by means of more innovative membranes prepared from new materials and applied in several fields of industries (Sagle & Freeman, 2004). Membrane technology is progressively becoming widespread for production of drinking water from different water sources. There are several types of membranes applied in water treatment processes. They consist of microfiltration (MF), ultrafiltration (UF), reverse osmosis (RO)

and nanofiltration (NF) membranes. Whereas, MF membrane has the largest pore size and usually remove big particles and several microorganisms. UF membrane has smaller pores than MF membranes and; therefore they can remove bacteria and soluble macromolecules (proteins). While, RO membranes are efficiently non-permeable, so, they remove particles and numerous low molar mass species (salt ions, organics etc.). NF membranes are result of recent development. They are permeable membranes, they also display efficiency and effectiveness in the middle of that of reverse osmosis and ultrafiltration membranes (Sagle and Freeman, (2004); Mazille and Spuhler,( 2012)). Figure 2 shows the Filtration spectrum of membrane technology.

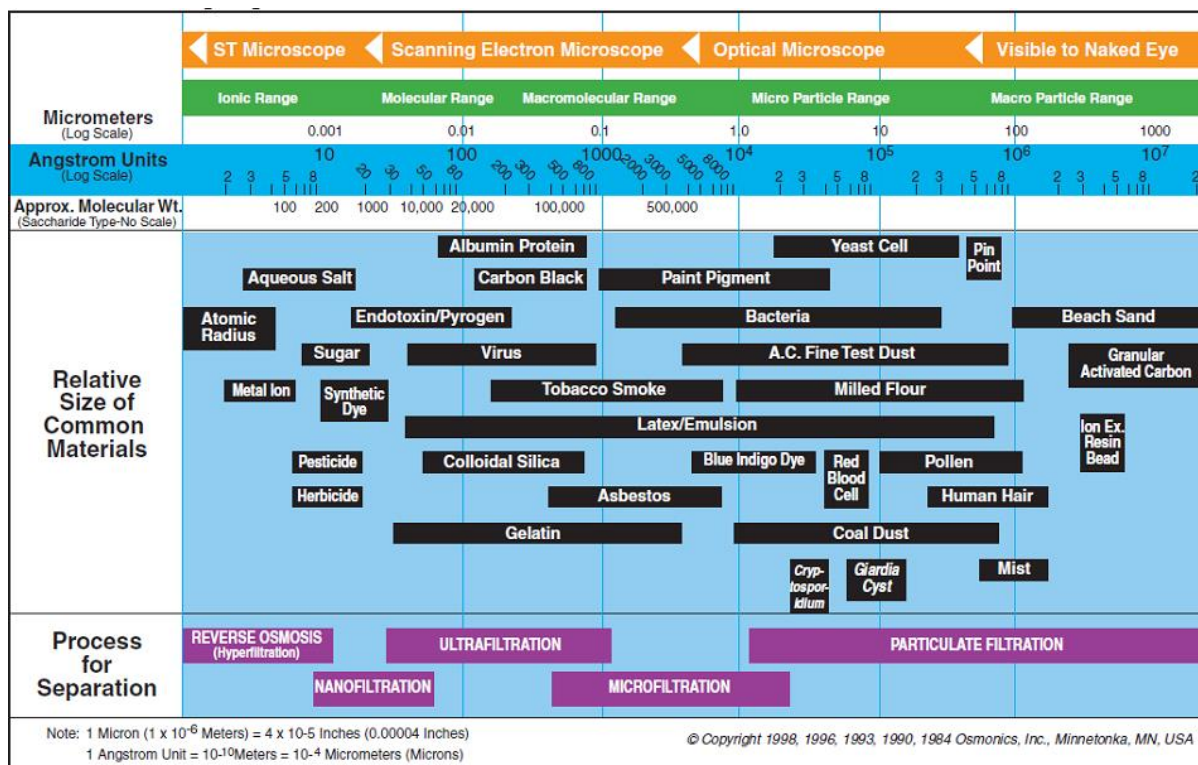


Figure 2: Filtration spectrum of membrane technology (Mazille & Spuhler, 2012).

## Electrodialysis (ED)

It is an applied technology that uses ion-exchange membranes to transport ions from one to another solution under the influence of an applied electric potential difference. In almost all applied ED applications, several ED cells are planned into a formation known as an ED stack, with anion and cation exchange membranes alteration, which forms the multiple ED cells (Strathmann, 2004) (Figure 3).

The efficiency of boron removal using ED have been investigated. At the best operational conditions, if the feed boron concentration in water is greater than 4.5 ppm, boron concentration cannot be reduced to 0.3- 0.5 ppm. Here, it is required to apply an further adjustment to the dialysate (Xu and Jiang, 2008).

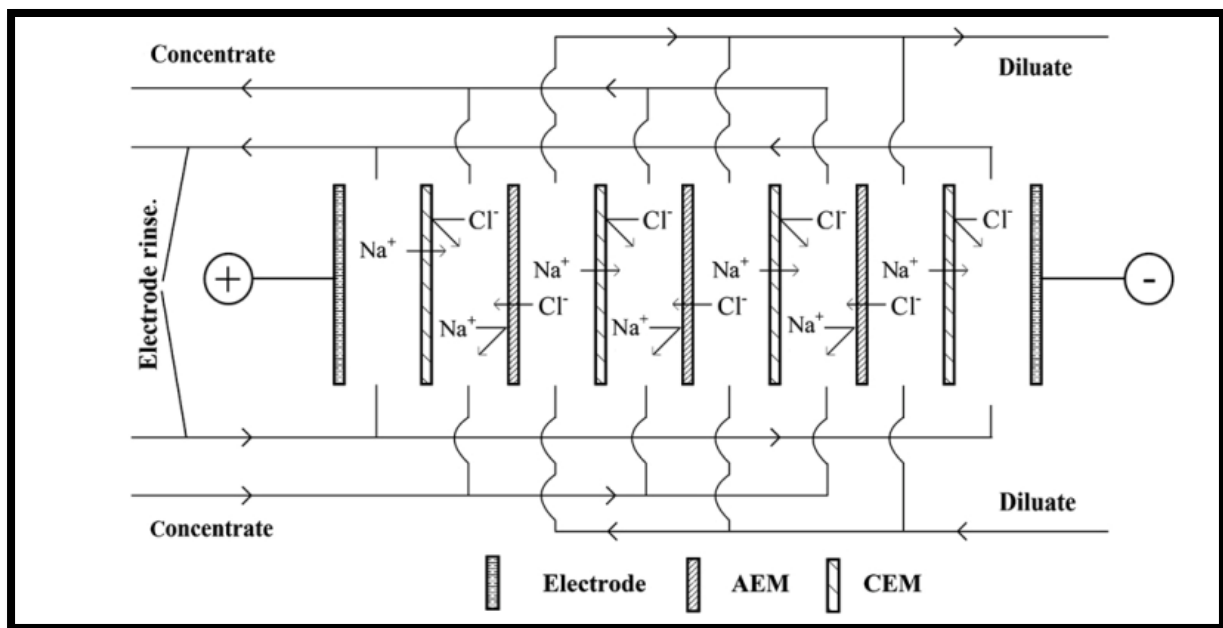


Figure 3: The scheme of ED separation of ionic species. Source: (Strathmann, 2004)

## Reverse Osmosis

Reverse osmosis (RO) is a water filtration technology that uses an effectively non-membrane to remove molecules, ions, and large size particles from water. Reverse osmosis

uses pressure to overcome osmotic pressure, which is a “molecules binding” characteristic that is instigated by a thermodynamic parameter which is the chemical potential differences of the solvent. RO can eliminate various sorts of dissolved and suspended species from water and is applied in industrial practices and the production of drinking water

When the feed water enters the RO membrane under applied pressure, the water molecules move through the effectively non-membrane and the salts and pollutants are not permitted to go though and are cleared through the reject stream, which either channeled to drain as discharge or can be recycled to feed stream to preserve water. Furthermore, the water that pass through the RO membrane is called permeate (product) water and typically has around 95- 99% removal (Güler et al., 2015). Figure 4 presents the Reverse Osmosis process diagram.

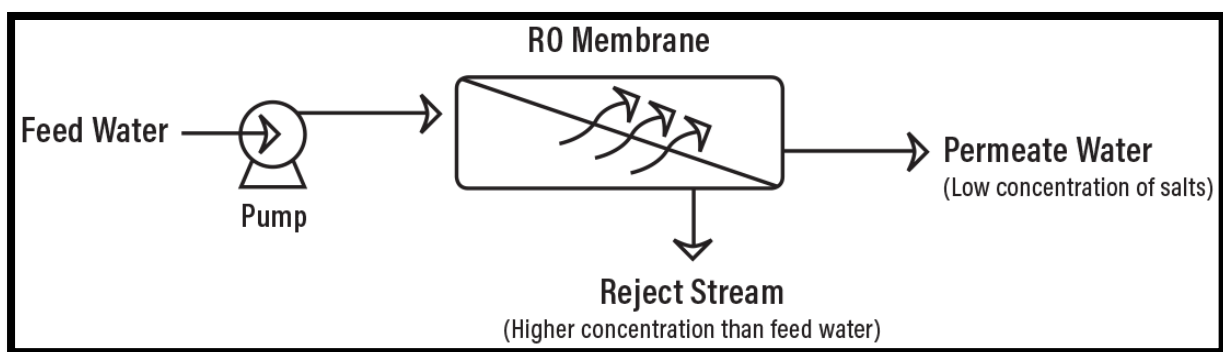


Figure 4: Reverse Osmosis process diagram. Source: (Güler et al., 2015).

Prats et al., (2000) showed that at pH ranges of 5.5–9.5, the rejection of  $B(OH)_3$  was reached to 40–60% while  $B(OH)_4^-$  removal was about 95%. Thus, the boron elimination by RO is reliant on the  $B(OH)_3/B(OH)_4^-$  ratio. With a high percentage of  $B(OH)_3$  in the feeding water will cause unacceptable levels of boron in the treated water. However, the existing RO membrane for boron treatment has the capability to treat boron for 85 to 90% which represents around 80% boron rejection at pH 8, 55.2 bar, 25°C. With the purpose of boron reduction in RO permeate and following the rigorous requirements, numerous technical

designs and concepts have been developed from the technical & economical aspect. However, the cost for typical water production is 0.38–0.50 \$/m<sup>3</sup> for 0.6–1 mg/L boron. Furthermore, the boron removal by RO is influenced by many causes, for instance, initial boron concentration, pH, temperature, flow rate, pressure and others. Therefore, it would be critical to observe a relationship between the boron removal percentage and the above-mentioned parameters.

### Selective Ion Exchange

It is mainly applied to soften the water when magnesium, calcium and other ions are present (US-EPA, 2014). There are two exchange process, cation & anion. In a cation exchange process, positively charged ions on the surface of the resin are exchanged with ones available on the resin surface. The water softening is the commonly applied cation exchange process. Likewise, in anion exchange negatively charged ions are exchanged with ones available on the resin surface; in which pollutants such as nitrate, fluoride, sulfate, and arsenic, as well as others, can all be removed by anion exchange (US-EPA, 2014).

Ion-exchange resin is an insoluble medium in the form of (0.25–0.5 mm radius) microbeads made from an organic polymer material. They are usually permeable with a large surface area. Furthermore, when the resin capacity is declined, it is recommended to regenerate the resin by applying saturated reagent to return the capacity of the resin to its best conditions (Figure 5) (US-EPA, 2014). Boron selective ion exchange resins are used to specifically target this pollutant. The media is a weakly basic resin (styrene resin with methyl glucamine functionality). Examples of boron selective resins include: Amberlite™ 743 (Rohm & Haas Company) and Dowex M4195 (Dow Chemicals Company). As with other ion selective treatment, boron selective resins employ traditional ion exchange system designs and operations. The exhausted resin is regenerated with sulfuric or hydrochloric (EPRI, 2007).

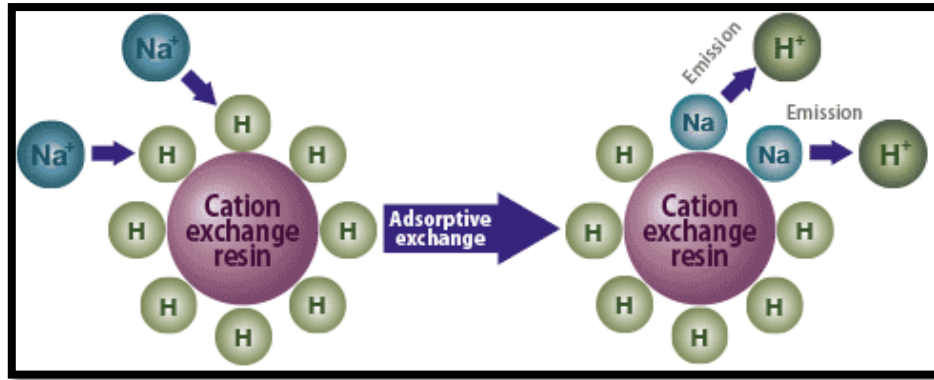


Figure 5: Types of Ion exchange resins (ASTOM, 2013).

Ion exchange membranes have ionic perm-selectivity and are classified into cation and anion exchange membranes. As negative charged groups are attached to cation exchange membrane, anions are excluded by the negative charge and cannot pass through the cation membrane (Figure 6-left). And the reasons is, cation exchange membranes are only permeable by cations. The anion exchange membranes function act on similar but opposite compared to cation membranes (Figure 6-right) (US-EPA, 2014). Boron remediation from aqueous media was investigated using Neosepta-AHA membrane by Donnan dialysis (DD) technique. Different key parameters were investigated such as concentration, membrane structure, conduct time, pH, and effect of others ions. It was established that the DD method is an effective method for remediation of boron from aqueous media when an suitable counter anion was selected at appropriate pH value (Ayyildiz and Kara, 2005).

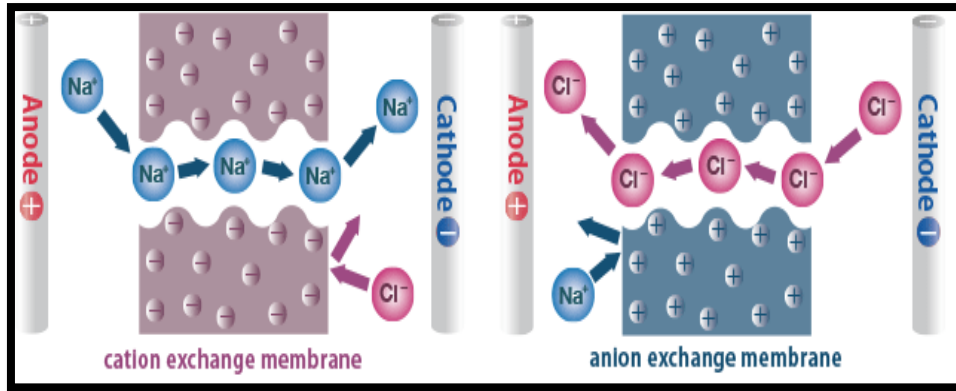


Figure 6: Types of Ion exchange membranes (ASTOM, 2013).

### Electro-coagulation

Electro-coagulation (EC) is an old technology that has found new interest in water treatment applications. The basic principles of this process are the same as those for conventional chemical precipitation with alum addition, except that a sacrificial electrode is used to generate the coagulates. The electric charge, imparted via the electrode, acts to neutralize the electrically charged colloidal particulates as well as oils present in the water (EPRI, 2007). As water penetrates the EC cell, several reactions occur simultaneously. First, on the cathode, water is hydrolyzed into H<sub>2</sub> and <sup>-</sup>OH. Then, electrons flow to destabilize surface charges on suspended solids and emulsified oils. Lately, bulky flocs form that entrain heavy metals and other contaminants. Lastly, the flocs are removed from the water in downstream solids separation and filtration process steps as illustrated in Figure 7.

There was a 35 month study to evaluate the viability of EC for the boron remediation from aqueous media. The study indicated that EC can successfully and economically remove boron. The effectiveness of boron remediation depends on the electrolytic time, initial concentration and the current density (Xu and Jiang, 2008).

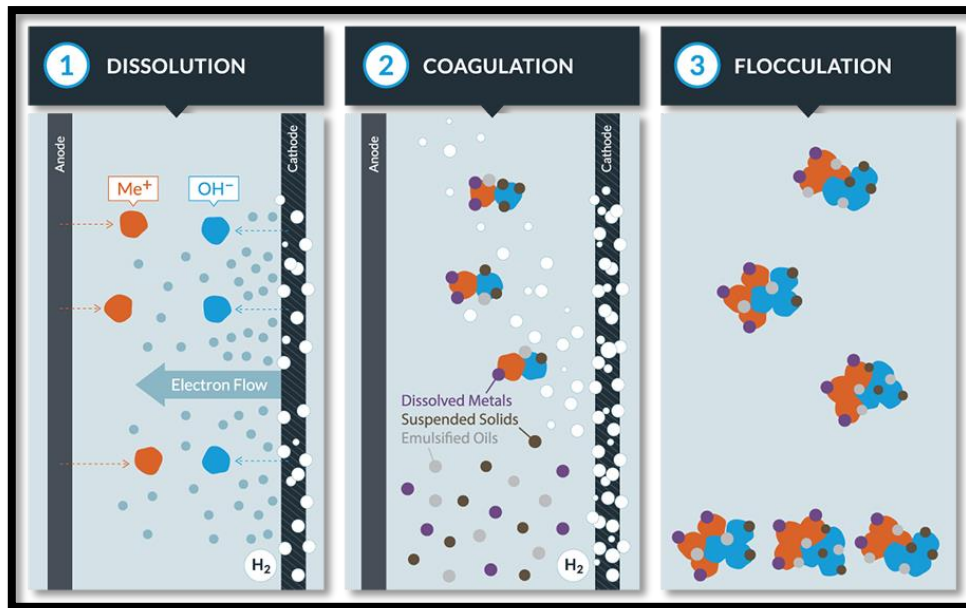


Figure 7: Electrocoagulation Process (WaterTectonics, 2017).

## Adsorption

There are two main components in any adsorption process; one is the adsorbent in which the adsorption takes place on and the second is the adsorbate, which the solute from a solution gets adsorbed on the adsorbent surface. Nonetheless, the characteristic of the forces presented between adsorbate molecules and adsorbent determines which type of adsorption, and it can be categorized into two categories (physical and chemical adsorption) as shown in Table 1 (Amrita institute of education, 2012).



*Table 1 Differences Between Physical & Chemical Adsorptions*

<b>Physical Adsorption</b>	<b>Chemical Adsorption</b>
Occur only at temperature below the boiling point of adsorbate	Occur at all temperature s
Heat of adsorption is below 40 KJ/mol	Heat of adsorption can be more than 200 KJ/mol
The adsorbed amount is increased when the pressure of adsorbate is increased	Pressure is insignificant
The adsorbed amount depend more on the nature of adsorbate than the adsorbent	The adsorbed amount depend on the nature of both adsorbate and adsorbent
No appreciable activation energy is required	appreciable activation energy may involve in the process
Multilayers adsorption occurs	Only monolayer adsorption occurs

Adsorption, using several common adsorbents, is considered as a useful and cost-effective, but relatively with a low capacity because of the weakly acidic boron compounds that would not bind strongly to the surface. The adsorption mechanisms would be by selectively boron adsorption and it is initiated by the formation of complexes. Various studies stated that boron adsorption via complexation will not be significantly interfered by the coexisting of salts. Though most of the adsorbents investigated in the literature are efficient in boron removal, they are expensive and generally difficult to prepare, which bounds their practical application in boron elimination from water (Weber et al., (1991); Karcher et al., (2001)).

In order to find a suitable adsorbent, there are criteria's that must be met: (i) high affinity and high adsorption capacity for the adsorbate (e.g. Boron); (ii) safe and

economically viable treatment; (iii) tolerance for a wide range of wastewater parameters; (iv) usable for all or nearly all boron, and (v) regeneration must be possible (Weber et al., 1991).

In adsorption, solute build-up is usually limited to the surface or boundary between the adsorbent and the solution. Here, solute is transported from one phase to another and penetrates the adsorbent phase. A variation of the process occurs if a high accumulation of solute adsorbs at the interface to form a precipitate or other type of molecular solute-solute association; forming new and distinct three-dimensional phases (Weber et al., (1991); Karcher et al., (2001)).

Solute solubility and its affinity for the solid are considered driving forces for adsorption. This kind of affinity may be predominantly one of electrical attraction of the solute to the adsorbent via van der Waals attraction or of a chemical nature. However, adsorption is recognized as a significant phenomenon in most natural processes including physical, biological and chemical.

Adsorption is an interface accumulation of an adsorbate species at an adsorbent surface. It can happen at the interface between any two phases, such as liquid-liquid, gas-solid or liquid-solid. The species being concentrated on the adsorbent is an adsorbate. At equilibrium, the adsorption process is thought to be at a dynamic state and the rate of the forward process is equal to the rate of the reverse process. Adsorbents used in adsorption processes usually have certain characteristics including: high specific surface areas for a unit mass, ranging between 100–1000 m<sup>2</sup>/g, high stability and availability at a relatively low price (Henning and Degel, (1990); Xu & Jiang,( 2008)). Figure 8 represents the fundamentals of the adsorption and desorption process on the adsorbent.

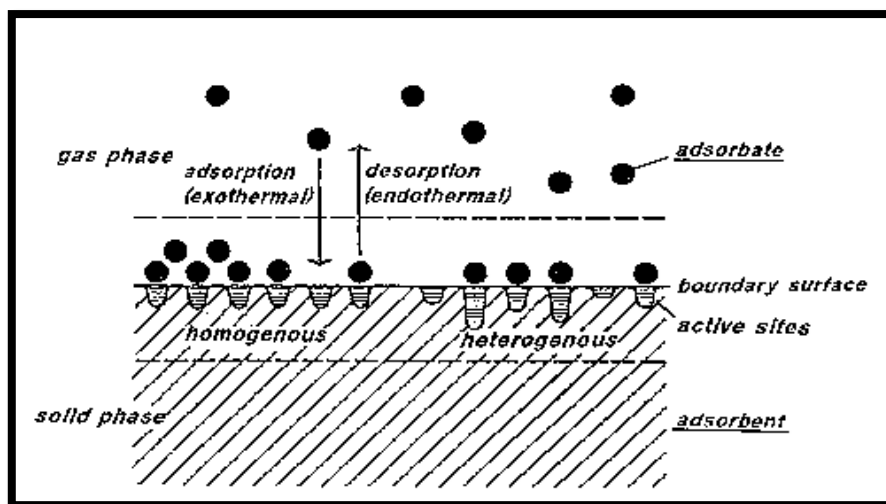


Figure 8 Fundamentals of adsorption and desorption process on the adsorbent .Source: (Henning & Degel, 1990).

According to a review study investigated by Xu & Jiang,( 2008), several technologies to eliminate boron concentration in water and wastewater were presented. The removal effectiveness and the evaluation for each technology are shown in Table 2.

Table 2 Removal Efficiency And Evaluation Of Various Technologies For Boron Removal

Technology	Boron remediation capacity	Comment
<b>Chemical precipitation</b>	60%	High sludge and salinity
<b>Ion exchange</b>	Very high at pH 12	Expensive
<b>Reverse osmosis</b>	<80% or very high when two stages will be used.	Saline wastewater
<b>Extraction [liquid-liquid]</b>	Very high	Expensive/solvent risk
<b>Electro-dialysis</b>	<80%	Expensive
<b>Electro-coagulation</b>	Very high, multistage should be used.	Expensive
<b>Adsorption [modified activated carbon]</b>	<70%	High investment

## Toxicity and benefit of boron

### Plants

Boron deficiency and toxicity have small margin in plant. Boron has been known to assist in several roles such as metabolism of carbohydrate, pollen germination, normal growth and others. Boron deficiency Indicators consist of leaf and root growth hindrance, fracturing of bark, delaying in enzyme reactions pollen, germination reduction, and others (Parks & Edwards, 2005). According to report of WHO (1998), the initial stages of boron toxicity in plants involve yellowing of leaf tips progressing into the leaf blade. Boron deficiency may take place in a high pH textured soil as boron is readily adsorbed under these conditions. Some plants are less tolerant to boron than others. Less tolerant plants can tolerate irrigation waters with only 0.3 ppm boron level, while very tolerant plants may be able to persist where 4 ppm boron level when irrigation water is applied (Parks & Edwards, 2005).

### Microorganisms

According to the study investigated by Bringmann & Kuhn (1980), the toxicity thresholds (TTs) for several microorganisms may vary. The TT for *Pseudomonas putidam*, *Scendesmus quadricauda*, and *Entosiphon sulcatum* were 290, 0.16 and 0.28 ppm boron; respectively.

### Animals

There are number of studies such as Hunt, (1994) and Hegsted et al., (1991) were found that boron is vital nutrient to animals. Boron have also exhibited ability to improve the development of the chick's long bones growth and rats brain activity impact. Many studies summarized extensively by Moore (1997), in which mice, rabbits, rats, dogs, and ducks were investigated. It was concluded that a no-observed-adverse-effect-level (NOAEL) of 9.6 mg

Boron/kg body weight/day was suitable on toxicity at the developmental stage of rats. Results showed NOAELs for male & female toxicity at the reproductive stage, were 24 and 17 mg/kg body weight/day, respectively.

## Humans

Due to not been able identify the biochemical function of boron, therefore, no evidence to the nutrition value to humans. Nonetheless, there is solid incidental indication that this may be true. There is indication that boron act in a role that effect joints & bones health. According to study carried out by Newnham, (1994, boron can be helpful in stopping and treating several arthritis types. There is no human evidence existing that successfully evaluate developmental toxicity. A number of studies shows the excursion of boron in urine. Janson and Schou, (1984) found that close to 98.7% of an injected 600-mg dose of boric acid was removed the first 5 days. Also, Oral doses have also been shown to be almost entirely eliminated in the urine by 92 to 94% was eliminated in the first 4 days.

## Adsorption isotherm

Adsorption process is typically investigated using adsorption isotherm graphs. In which, the quantity of adsorbate attached to the adsorbent as a function if its pressure/concentration at constant temperature (Garg et al., (2008); Allen et al., (2004)). Figure 9 shows a typical adsorption Isotherm (Amrita institute of education, 2012).

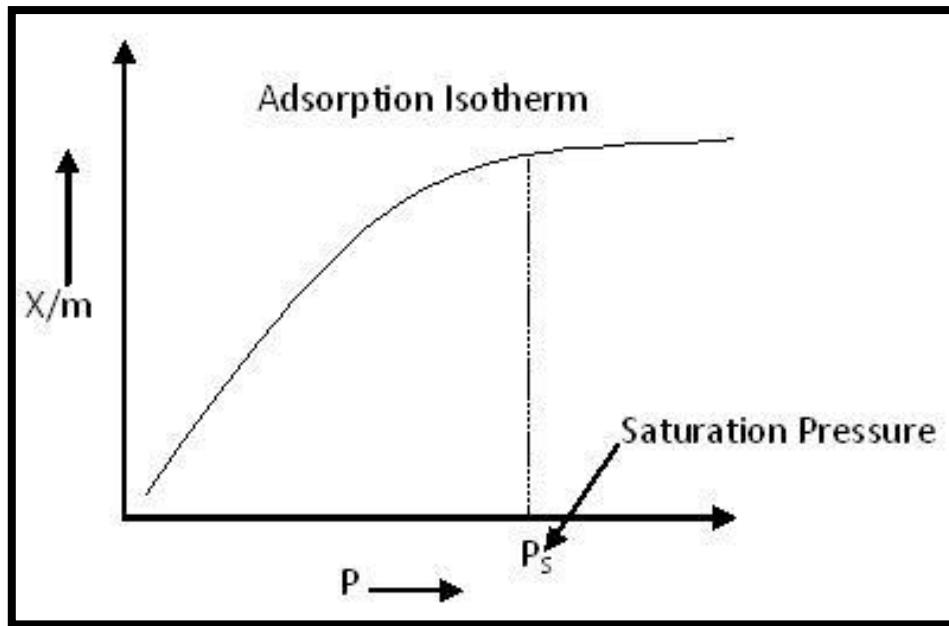


Figure 9: Adsorption Isotherm. Source:(Amrita institute of education, 2012)

Adsorption isotherms are also related to the amount of substance adsorbed by an adsorbent to the equilibrium concentration of that substance at constant temperature. Six general types of isotherms have been observed as illustrated in Figure 10. When the adsorption rate matches the desorption rate, equilibrium has been achieved and the capacity of the adsorbent has been reached. The theoretical adsorption capacity/amount of adsorbed containment at equilibrium of the adsorbent can be achieved by applying well-known adsorption isotherm models (Foo and Hameed, 2010). Figure 10 presents the classification of adsorption isotherms defined by IUPAC.

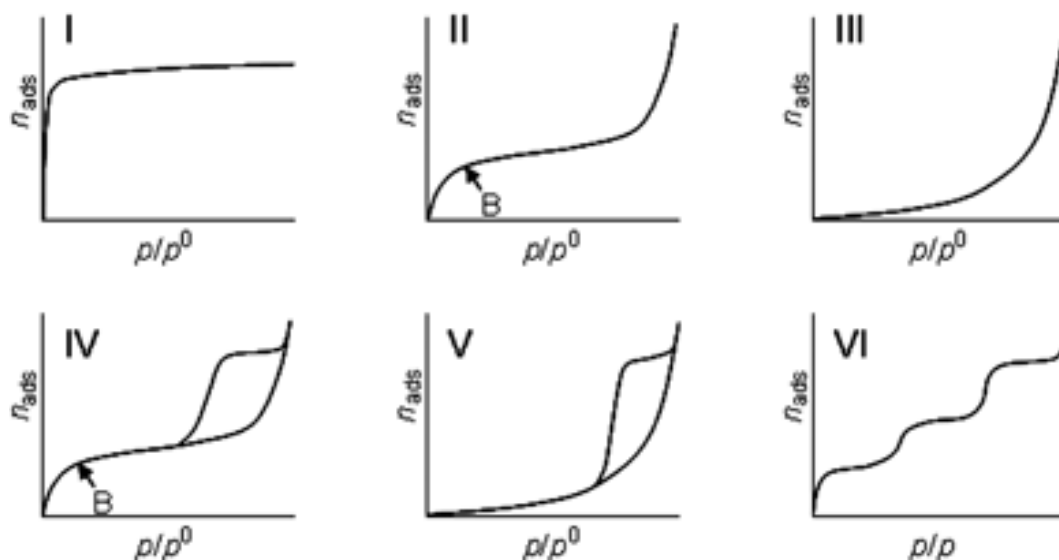


Figure 10: Classification of adsorption isotherms (Amrita institute of education, 2012). I: Micro porous Materials; II: Non porous Materials; III: Non porous materials and materials which have the weak interaction between the adsorbate and adsorbent; IV: Mesoporous materials; V: Porous materials and materials that have the weak interaction between the adsorbate and adsorbent and VI: Homogeneous surface materials

### Isotherm models

An adsorption isotherm is a curve indicating the occurrence governing the release of a constituent from the aqueous permeable media to a solid phase at a constant temperature. A wide-ranging assortment of isotherm models (such as Langmuir, Freundlich and others) have been expressed in terms of three fundamental approaches; namely (i) kinetic consideration (dynamic equilibrium: adsorption equals desorption rates), (ii) thermodynamics offer an outline to originate many adsorption models, and (iii) the potential theory that helps in the generating the characteristic curve (Foo and Hameed, (2010); Garg et al., (2008); Allen et al., (2004)).

The first step in an efficient adsorption process is the search for an adsorbent with high selectivity, high adsorption capacity and long life. The selectivity of adsorbents is measured by: (i) equilibrium studies (capacity of adsorbent, or the dosage required to remove a unite mass of pollutant), (ii) kinetic studies (the rate of adsorption, the time elapsed before a given concentration of solute is removed from solution and (iii) molecular sieve separation (Zalloum et al., 2008).

Adsorption is the removal of a solute from a solution, and the concentration of the solute continuing in solution is in a dynamic equilibrium with that at the surface. Consequently, a distribution of the solute between the liquid and the solid phases will be exist. This distribution is expressed by the quantity  $q_e$  as a function of  $C_e$  at fixed temperature as described in equation 1 (Aisien et al., (2013); Taimur & Malay, (2011)).

$$q_e = \frac{(C_o - C_e)V}{m} \dots\dots\dots\text{Eq.1}$$

$q_e$  is the amount of adsorbate adsorbed per unit weight of solid adsorbent,  $C_o$  is the initial concentration of adsorbate (mg/L),  $C_e$  is the equilibrium concentration of adsorbate (mg/L),  $V$  is the volume of liquid (L) and  $m$  is the mass of adsorbent (g). Langmuir and Freundlich isotherm models were used to describe the adsorption isotherms of boron.

*The Langmuir isotherm model*

The Langmuir model was initially established to define solid/gas stage sorption to activated carbon. It has also usually been applied to measure and compare bio-adsorbents performance. This model indicate adsorption at the monolayer level, with adsorption transpiring only at limited localized sites, that are similar, with no crosswise interaction and atoms spatial arrangement interference amidst the adsorbed molecules. Langmuir isotherm, in its derivation form indicates a homogeneous adsorption, in which all sites retain equivalent attraction for the adsorbate. Graphically, it is characterized by an a state of little/no change



( saturation point) subsequent no further adsorption can take place (Foo & Hameed, (2010); Garg et al., (2008); Allen et al., (2004)).

The Langmuir isotherm predicts the existence of monolayer coverage of the adsorbate at the outer surface of the adsorbent. The linear form of Langmuir adsorption isotherm is given equation 2: (Christmann, (2012); Moghaddasi et al., (2013)):

$$\frac{1}{q_e} = \frac{1}{Q^\circ b} x \frac{1}{C_e} + \frac{1}{Q^\circ} \dots\dots\dots\text{Eq.2}$$

Where  $Q^\circ$  and  $b$  are Langmuir constants representing the measure of adsorption capacity of monolayer (mg/g) and affinity of adsorbent towards adsorbate. The plot between  $1/q_e$  and  $1/C_e$  is a straight line with a slope of  $1/Q^\circ b$  and intercept of  $1/Q^\circ$ .

The Langmuir constant,  $b$ , along with initial concentration,  $C_0$ , was used to calculate the separation factor,  $R_L$ , using the equation 3. The dependency of the nature of adsorption on the value of  $R_L$  is presented in Table 3.

$$R_L = \frac{1}{1+bC_0} \dots\dots\dots\text{Eq.3}$$

*Table 3:  $R_L$  Values And Type Of Isotherm* (Aisien Et Al., 2013; Karthikeyan and Siva Ilango, 2008).

<b><math>R_L</math></b>	<b>Type of isotherm</b>
$R_L > 1$	Not favorable
$R_L = 1$	Linear
$1 < R_L < 0$	Favorable
$R_L = 0$	Not reversible

*The Freundlich isotherm model*

The Freundlich model was initially established to define reversible & non-ideal adsorption, also not limited to the formation at monolayer level. This model is used to describe sorption at the multilayer level, with (not-uniform) heterogeneous distribution of adsorption affinities and heat at the heterogeneous surface. Therefore, the sum of all sites adsorption equals, the amount adsorbed, with the binding sites which are stronger are first occupied, till energy of adsorption are decreased exponentially on the adsorption process completion (Ahmaruzzaman, 2008). In addition, heterogeneous systems is broadly represented by Freundlich isotherm, particularly the case for highly interactive species at activated carbon (AC) organic compounds. In this isotherm model, the range of (0-1) is a surface heterogeneity adsorption intensity index; when the value gets closer to zero, it will be characterized as more heterogeneous. While, a value below (1) indicates a chemical adsorption, whereas a value of  $1/n$  more than one, it signifies of supportive adsorption (Haghseresht and Lu, 1998).

According to (Foo & Hameed,(2010) ; Gupta & Babu, (2009)), Freundlich model explains the multilayer adsorption on heterogeneous surfaces, through the equation 4:

$$q_e = K_f x C_e^{1/n} \dots\dots\dots \text{Eq.4}$$

The linear form of the equation was obtained by taking logarithm on both the sides is given in equation 5:

$$\log q_e = \log K_f + \left(\frac{1}{n}\right) * \log C_e \dots\dots\dots \text{Eq.5}$$

A straight line was obtained as a result of plot between  $\log q_e$  and  $\log C_e$  with a slope and intercept of  $1/n$  and  $K_f$ , respectively.

## Kinetic studies

### Pseudo first order kinetic model

The pseudo first order kinetic model can be expressed in equation 6, as:

$$\frac{1}{qt} = \left(\frac{k_1}{q_1}\right) * \left(\frac{1}{t}\right) + \frac{1}{q_1} \dots\dots\dots\text{Eq.6}$$

Where  $q_t$  is the amount of boron adsorbed (mg/g) at time  $t$ ,  $q_1$  is the maximum adsorption capacity (mg/g) for pseudo first order adsorption,  $k_1$  is the pseudo first order rate constant for the boron adsorption process ( $\text{min}^{-1}$ )(Aisien et al., 2013). The linear form of pseudo first order equation is given in equation 7, as:

$$\ln(Q_e - Q_t) = \ln Q_e - k_1 t \dots\dots\dots\text{Eq.7}$$

With experimental data of  $Q_t$  and  $t$ ,  $Q_e$  and  $k_1$  are obtained as adjustable parameters from curve fitting. It is difficult to extract  $Q_e$ , because it gives a relation between  $\ln(Q_e - Q_t)$  and  $t$ . So, there is need to assume a value of  $Q_e$  experimental (by trial and error, but keeping the value close to the experimental  $Q_e$ ) and looking for the best regression coefficient when fitting in the experimental data. After plotting  $\ln(Q_e - Q_t)$  and  $t$ , the  $Q_e$  calculated is compared to experimental  $Q_e$  (the one used in  $\ln(Q_e - Q_t)$ ). If it does not equal in all contact time ranges, then pseudo first order kinetic model does not fit with batch study.

### Pseudo second order

The pseudo second order kinetic model can be expressed in equation 8, as:

$$\frac{t}{qt} = \frac{1}{k_2 * q_2} + \frac{t}{q_2} \dots\dots\dots\text{Eq.8}$$

Where  $q_t$  is the amount of boron adsorbed (mg/g) at time  $t$ ,  $q_2$  is the maximum adsorption capacity for the pseudo second order adsorption (g/mg min),  $k_2$  is the pseudo second order rate constant ( $\text{min}^{-1}$ ) (Yüksel and Yürüm, 2009).

In general, due to its simplicity, the pseudo second-order kinetic has been widely applied in the designing of very adsorption methods. Since the pseudo second-order is nonlinear, seem that appraising the value of  $q_e$  and the rate constant of adsorption  $k$  needs adjusting the equation to empirically result by nonlinear of regression applying methods of numeric optimization. A proper choice for non-linear of regression is to apply linearized variants of the equations that the pseudo second-order kinetic could be linearized to four versions (Table 4) for the calculation of parameters of  $q_e$  and  $k$  (Ghasemi et al., 2013).

Table 4: Pseudo Second -Order Kinetic Be Linearized Versions

Linearized versions	Linear Equation	Plot	Parameters
1	$\frac{t}{qt} = \frac{1}{k_2 \times q_e^2} + \frac{t}{q^2}$	$\frac{t}{qt} = t$	$q_e = 1/\text{slope}$ , $K_2 = (\text{slope}^2)/\text{intercept}$
2	$\frac{1}{qt} = \frac{1}{q_e} + \frac{1}{Kq_e^2} \times \frac{1}{t} + \frac{1}{q_e}$	$\frac{t}{qt} = \frac{1}{t}$	$q_e = 1/\text{intercept}$ , $K_2 = (\text{intercept}^2)/\text{slope}$
3	$\frac{1}{t} = \frac{k_2 \times q_e^2}{qt} - \frac{k_2 \times q_e^2}{q_e}$	$\frac{1}{t} = \frac{1}{qt}$	$q_e = -\text{slope}/\text{intercept}$ , $K_2 = (\text{intercept}^2)/\text{slope}$
4	$\frac{q}{t} = k_2 \times q_e^2 - \frac{k_2 \times q_e^2 \times qt}{q_e}$	$\frac{q}{t} = qt$	$q_e = -\text{intercept}/\text{slope}$ , $K_2 = (\text{slope}^2)/\text{intercept}$

## Elovich model

This model assumes that the adsorption sites increase exponentially with adsorption, which implies a multilayer adsorption (Farouq & Yousef, 2014; El-Sherif et al., 2013). The Elovich equation, which is given by in equation 9, as:

$$\frac{dq_t}{dt} = \alpha * \exp(-\beta q_t) \dots\dots\dots \text{Eq.9}$$

Where  $\alpha$  and  $\beta$  are constants during any an experiment. The constants  $\alpha$  and  $\beta$  were obtained from the slope and intercept of the linear plot of  $q_t$  versus  $\ln t$ . The constant  $\alpha$  is regarded as the initial rate because  $(dq_t/dt)$  approaches  $\alpha$  when  $q_t$  approaches 0.

By applying the boundary conditions  $q_t = 0$  at  $t = 0$  and  $q_t = q_t$  at  $t = t$ , the integrated form is:

$$q_t = \frac{1}{\beta} \times \ln(\alpha\beta) + \frac{1}{\beta} \times \ln(t)$$

The plot of  $q_t$  vs.  $\ln(t)$  should yield a linear relationship with a slope of  $(1/\beta)$  and an intercept of  $(1/\beta) \ln(\alpha\beta)$  (Tutu et al., 2013).

The average relative error deviation (ARED) is the minimization of the fractional error distribution across the entire concentration range as shown in equation 10 (Chan et al., 2012).

$$ARED = \frac{1}{N} \sum \left( \frac{Q_c - Q_e}{Q_e} \right) \times 100 \dots\dots\dots \text{Eq.10}$$

Where  $N$  is the number of experimental data points,  $q_c$  (mg/g) is the theoretically calculated adsorption capacity at equilibrium and  $q_e$  (mg/g) is the experimental adsorption capacity at equilibrium (Riahi et al., 2013).

## Waste Management of Tire

Waste management is an important topic. The quantity of waste is considerably rising for many years all over the world. The tires disposal shows a key environmental concern in many countries. Consequently, the management of waste tire has turn out to be a great concern (Rungronmitchai and Kotatha, (2015)a; Gonzalez et al., (2001)). Build up stocks of tires deliver perfect habitat for species which are known for disease vectors such as rodents, insects. There are also the danger of accidental fires in tire dump sites, which cause release of toxic fumes.

There are several method of waste tire disposal such as landfill, energy recovery, and reutilization in sports surfaces and roofing materials. However, most of the countries firmly bans the disposal of waste tire on landfill and use them as a fuel because of the environmental problems that may arise owing to the emission of hazardous pollutants. The structures of the waste tire contains double bonds which are useful for chemical modification that are derived from isoprene units of natural rubber and butadiene polymer units of synthetic rubber (Rungronmitchai and Kotatha,( 2015)a; Kim et al., (1997)) .

## Waste Tire as Adsorbent

Tires are made of vulcanized rubber, rubberized textile having strengthening fabric strings, steel or steel-wire-reinforced rubber heads and fabric belts; where styrene-butadiene rubber (SBS) is the widest used components in tires (60-65%). Additives such as carbon black (29–31%), extended oil, sulfur (1-2%), zinc oxide (2-3%), and stearic acid were added to tires in order to enhance their performance (Kim et al., 1997; Cunliffe and Williams, 1998). Furthermore, various investigators studied the proximate and ultimate analysis of waste tires and the results are shown in Tables 5 and 6.

Table 5: Analysis Of Waste Tire Rubber (Aisien et al., 2013).

Characteristics	Value (wt %) at Reference		
	(Aisien et al., 2013).	(Lee et al., 1995)	(Gonzalez et al., 2001)
<b>Fixed Carbon</b>	28.35	28.5	29.2
<b>Moisture</b>	0.51	0.5	0.7
<b>Ash</b>	7.6	3.7	8
<b>Volatile</b>	63.54	67.3	61.9

Table 6: Ultimate Elemental Analysis Of Waste Tire Rubber(Aisien Et Al., 2013).

Characteristics	(Aisien et al., 2013)	(Cunliffe and Williams, 1998)	(Manchon Vizueté et al., 2004)
<b>Carbon</b>	86.5	86.4	86.7
<b>Hydrogen</b>	6.64	8	8.1
<b>Oxygen</b>	1.1	3.4	1.3
<b>Nitrogen</b>	0.4	0.5	0.4
<b>Sulfur</b>	2	1.7	1.4
<b>Inorganic Ash</b>	2.85	2.4	2.9

The application WTR as adsorbent in wastewater treatment is applied at several shapes and types; specifically granules, chips, rubber, ash and tire derived activated carbon and others. Kim et al., 1997 described the adsorption capacity at equilibrium of WTRG for

some substances. They concluded that m-xylene presented the top partition coefficient (977 L/kg), then followed by decreasing order by (ethylbenzene, toluene, trichloroethylene, 1, 1, 1-trichloroethylene, and chloroform), and the minimum is methylene chloride with value of 13 L/kg. Furthermore, it was observed that the organic compounds were adsorbed predominantly onto polymeric molecules of WTR. The study concluded that the WTRG presented excellent adaption capacity for organic compounds. Smith et al., 2001 applied chips of WTR to adsorb water containing phenol and p-cresol. They stated that the tire chips showed a great potential for integration in a permeable barrier.

Tires are good adsorbent mainly due to the presence of carbon black which account for 29–31% total tire, and they have similar chemical composition to activated carbon. Furthermore, the presence of styrene-butadiene rubber (SBS) which account 60-65% of total tire showed a significant adsorption capability to organic compounds in portable water distribution systems (Kim et al., 1997).

#### Why use chemically modified WTR & Nano-WTR

One of the problems with the applications of WT are the low adsorption capacity and slow adsorption kinetics. Therefore, in order to enhance the effectiveness of WT for boron removal, a chemical surface-modification and a nanoparticle of waste tires (WT) were produced and investigated in this project. This would help to fully understand the adsorption mechanisms and propose low-cost and easily obtainable adsorbents for boron removal.

#### *Chemical modification of WTR*

According to Alam et al., (2006), the pre-treatment of WTR by distilled water should be carried out. After that, the sample must be cut to pieces with the help of a cutting tool such as hacksaw and furthermore to small pieces using very sharp cutting tool.



Rungrodnimitchai and Kotatha, 2015b prepared Ethylenediamine (ETD) modified ground tire rubber for nitrate ion removal as shown in the Figure 11. The ETD modified ground tire rubber was composed of insoluble site from ground tire rubber and chloride ions as ion exchangeable site in the structure. The ETD modified ground tire rubber works by exchanging anions such as  $\text{NO}_3^-$  in the aqueous solution with chloride.

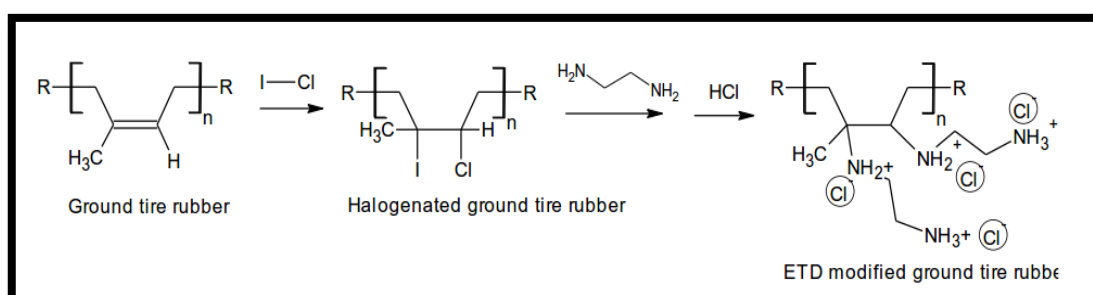


Figure 11: Reactions for preparation of the modified ground tire rubber; halogenation of carbon-carbon double bond, Aminolysis of halogenated ground tire rubber, followed by treatment by HCl to yield ETD modified ground tire rubber. Source : (Rungrodnimitchai & Kotatha, 2015b).

Rungrodnimitchai and Kotatha, (2015) produced a modified tire rubber (TR) that can be used as anion exchange resin for fluoride removal. It was carried out through a reaction with bromine and ethylene diamine in a microwave heating. Here, ethylene diamine was introduced into the TR structure; this was followed by protonation in an acid solution as shown in the Figure 12.

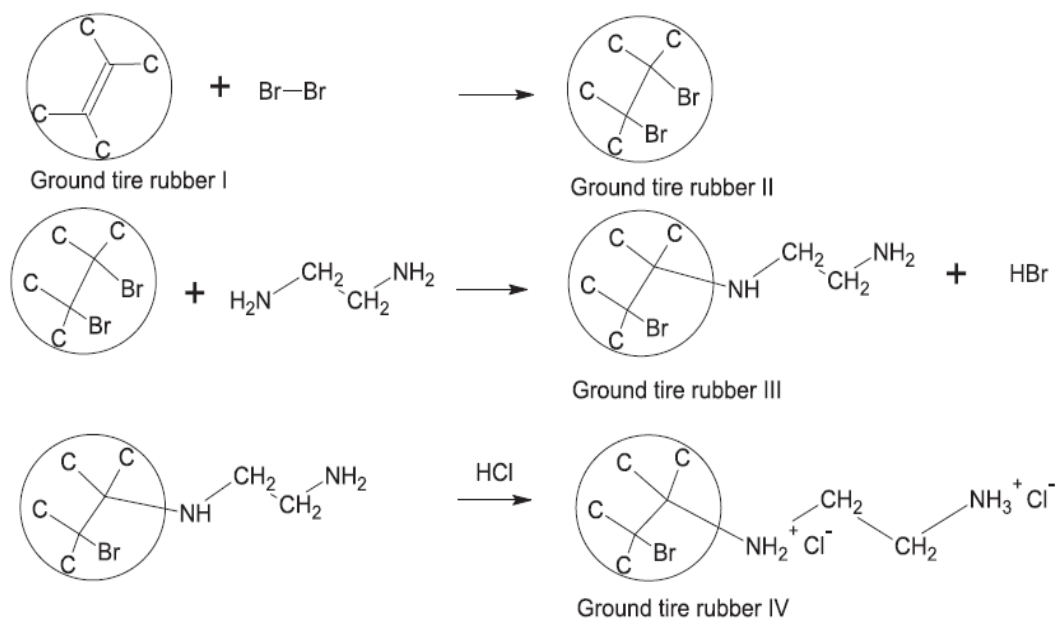


Figure 12 Reactions for preparation of the modified WTR ;(1) Bromination of carbon-carbon double bond, (2) Aminolysis of dibromide product, and (3) Protonation of Ethylenediamine modified WTR. Source : (Rungrodnimitchai & Kotatha, 2015b)

### *Nano-WTR*

Moghaddasi et al., (2013) prepared nanoparticles from WTR by the following procedure: The rubber particles was grounded using a ball mill for 5 hours with and without addition of liquid nitrogen. In addition, they used a combination with silicon wastes for 5 hours and they were successfully converted tire rubbers into the <100 nm-size particles. Li et al., 2017 prepared MgO nano-sheets using ultrasonic method with Mg(NO<sub>3</sub>)<sub>2</sub> solution. In summary, Table 7 summarizes different authors activities in using WTR as adsorbent.

*Table 7 Results of published citations on application of WTR as adsorbent*

<b>References</b>	<b>Investigation</b>	<b>Conclusion</b>
(Rungrodmitchai & Kotatha, 2015a)	Investigated the phenol elimination of wastewater using nanoparticles of WT	It was concluded that smaller particles presented excellent enhancement for the phenol adsorption.
(Rungrodmitchai & Kotatha, 2015b)	Investigated the Adsorption of mercury by CA prepared from WTR.	It was concluded that the ability to adsorb mercury is higher for the heated products than for the chemically-treated ones.
(Imyim et al., 2016)	Investigated the Arsenite and arsenate removal from waste-water using cationic polymer-modified WT.	It was concluded that As (V) could be adsorbed on to the sorbent more effectively than As (III). Remarkable desorption of As (III) and As (V) (99 and 92%, respectively) from the adsorbent was achieved using 0.10 M HCl as effluent.
(Aisien et al., 2013)	Investigated the Adsorption of Ethylbenzene from Aqueous Solution Using WTR.	It was concluded that results achieved lead to that WTR can be applied as an efficient adsorbent for the removal of Ethylbenzene.

Why use FTIR, SEM/EDX and CHN/O to characterize WTR

Understanding the mechanism of boron remediation onto WTR is essential for the removal of boron from effluents. In addition, understanding the mechanism of adsorbent-boron interaction can lead to the better prediction and description of the boron adsorption system. Moreover, the knowledge of the mechanism of adsorption might assist in the identifying of the optimal chemical treatment of the surface of an adsorbent to improve the boron adsorption potential (Zalloum et al., 2008).

The adsorbent surface chemistry and its effect on the overall adsorption process were examined. Fourier transform infrared (FTIR) method provides an unrivalled method for the characterization of the surface-adsorbate interactions. In general, the FTIR method for characterization of physical adsorption involves the observation of perturbations of surface groups or of adsorbed molecules. Chemisorption is recognized by the appearance of infrared bands due to vibrations of the products of adsorption (Al-Ghouti et al., 2003).

### Chapter 3: Materials and Methods

#### Preparation of Adsorbent

The waste tire rubber (WTR) was collected from Qatar's Domestic Solid Waste Management Department; the tire dump site in Doha City, Qatar. The tires was then cut into relatively small pieces and washed with water in order to remove dirt. The sample was then air dried. The WTR was then cut into very small pieces using electric a shredder machine. The resulting particles were sieved into several particles sizes in the range of 1 mm – 125  $\mu\text{m}$ . The sieved particles was then washed with distilled water in mechanical shaker for 3 hours and dried in oven for 5 hours at 60°C. Figure 13 shows the preparation steps of the WTR.

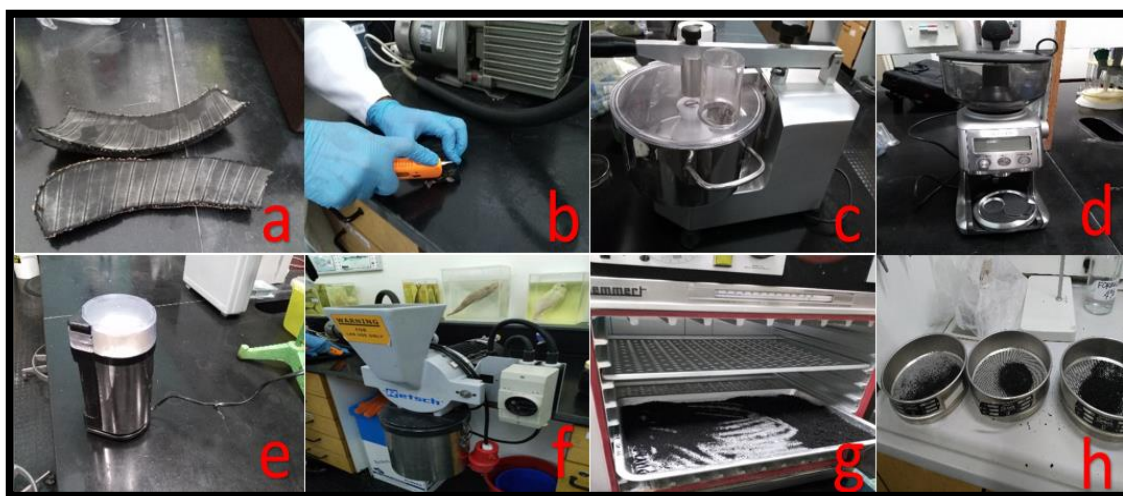


Figure 13 Preparation of Adsorbent, whereas a: cutting tire by hacksaw; cutting by knife, etc.; c-f: shredding & grinding to micro-size; g: dry at oven after cleaning; and h: sieving WTR

## Preparation of Standard Solutions

The stock solution of boron (measured as 200 mg/L) was prepared from analytical grade of  $\text{H}_3\text{BO}_3$ . Appropriate solutions were freshly arranged by using  $\text{H}_3\text{BO}_3$  stock solution with a distilled water prior to adsorption experiments.

## Chemicals

Anhydrous boric acid ( $\text{H}_3\text{BO}_3$ ), obtained from Reidel-de Haen Company (Germany), was used in this project. Hydrochloric acid, nitric acid and sulfuric acid (Merck grade), and sodium hydroxide (Merck grade) were also used.

## Preparation of nano-particles from WTR

After shredding the WTR into small pieces, their sizes were then reduced through multiple successively finer blade shredders to further reduce shreds into smaller particles. Then they were treated to smaller particles by grinding rolling mills. The particles were then sieved on sieves with different screen mesh. For nanoparticles preparation, the particles were milled at high speed with liquid nitrogen to increase the efficacy of milling. The sizes of the nanoparticles were then examined qualitatively using scanning electron (SEM).

## Preparation of chemically treated WTR and nano-WTR

In the chemical treatments, 10 g of the adsorbent is reacted with the acid solution (1 acid: 1 water by volume).  $\text{H}_2\text{SO}_4$  or  $\text{HNO}_3$  or a mixture of acids are used. The  $\text{H}_2\text{SO}_4/\text{HNO}_3$  mixtures are the following ratios (1:3), (3:1), and (1:1). Then, the treatment was carried out by immersion of WTR samples for 24 hours in  $\text{H}_2\text{SO}_4/\text{HNO}_3$  mixtures solutions. The treatment was followed air drying for 5 min, neutralization with 3.0 M NaOH and rinsing the sample with distilled water at room temperature until pH reach 7.

## Characterization of the adsorbents

### Fourier Transform Infrared (FTIR)

The FTIR spectra of the WTR, nano-WTR, and its modified forms were recorded using the (FT-IR Spectrometer Frontier/ TGA 4000 – Perkin Elmer). The FTIR analysis was carried out to interpret the functional groups which occurred in the adsorbents. The FTIR measurements were performed over 4000–400  $\text{cm}^{-1}$ .

### Scanning electron microscope (SEM)/EDX

Scanning electron microscope (SEM) (FEI Quanta 200 Environmental Scanning Electron Microscope (ESEM)) was also used to evaluate the surface morphology of the adsorbents and also using EDAX (EDS microanalysis system) for elemental analysis. The sample surfaces were sputter-coated with gold powder for SEM.

### CHN/O elemental analyzer

The chemical composition of the adsorbents is also studied using (CHNS/O analyzer - Perkin Elmer 2400).

## Experimental Procedure – Batch Adsorption test and Isotherm study

### Batch Adsorption

Adsorption remediation experiments was performed in order to obtain information about the equilibrium boron data and examine various parameters such as adsorbent dosage, pH, initial concentration, particle size and contact time and on boron removal in the laboratory batch unit. A stock solution (50 mg/L) of boron was prepared by dissolving a suitable amount of  $\text{H}_3\text{BO}_3$ . All solutions is prepared with distilled water. 0.05 g of the

adsorbent was thoroughly mixed with 50 mL of these solutions in 100 mL cleaned polythene bottles using mechanical shaker (Innova 2100- Platform Shaker) for 48 hours at constant speed of 150 RPM at room temperature ( $25\pm 1^\circ$  C). The bottles were agitated until equilibrium was attained. Then, the solution is filtered-out using 10 cm<sup>3</sup> syringe and analyzed for boron concentration.

#### Analysis of Samples

The boron analysis was carried out using the inductively coupled plasma– optical emission spectrometry (ICP-OES) (Thermo Scientific - iCAP 6300 - ICP-OES CID Spectrometer). Here, a special care is taken into considerations when the boron water samples were collected and stored for the boron analysis as the water samples can be contaminated by borosilicate glass. Only plastic materials are used.

#### Parameters of the study

##### *pH*

To examine the effect of pH, 21 samples of boric acid solutions (50 mg/L) is prepared at different pH values (2, 4, 6, 7, 8, 10 and 12) in triplicates. After finding the pH value with highest adsorption, the optimum pH value was used in all the remaining experiments (initial concentration, adsorbent dosage and particle size).

##### *Adsorbent dosage*

To examine the effect of adsorbent dosage, 18 samples of boric acid solutions (50 mg/L) is prepared at different adsorbent dosage (0.5, 1, 1.5, 2.0, 2.5, 3.0 g) in triplicates. The adsorbent dosage was applied for WTR only.



### *Initial concentration*

To examine the effect of initial concentration, 27 samples of boric acid solutions are prepared at different values (0(control), 5, 10, 20, 30, 70, 80, 90, 100 mg/L) in triplicates. The initial concentration study was applied for WTR, chemically modified WTR and Nano-WTR.

### *Adsorbent particle size*

To examine the effect of adsorbent particle size, 9 samples of boric acid solutions are prepared at different adsorbent particle sizes (125-250, 250-500, 500-1000  $\mu\text{m}$ ) in triplicates. The adsorbent particle size was applied for WT only.

### Experimental Procedure – kinetic studies

A specific weight of the adsorbent and boron concentration was agitated in a 2 L beaker for a satisfactory period of time to enable the system to approach equilibrium. Different time intervals (1 min, 5 min, 10 min, 15 min, 30 min, 1 hour and 2 hours) and adsorbent weight (1 g, 1.5 g and 2 g of adsorbent) were applied for each session. For the adsorption kinetic experiments, different kinetic models are applied, namely Lagergren pseudo-first and pseudo-second-order, and Elovich equation.

### WTR Leachability test

In order to investigate the metal leachability from the WTR, one gram of the WTR was contacted with distilled water at different pH values (2, 4, 6, 8, and 10) using a mechanical shaker for 24 hours at a constant speed of 150 RPM. The bottles were then agitated until equilibrium was achieved. Then, different metal concentrations (Pb, Zn, Cd, Fe,

B, and Cr) are measured using inductively coupled plasma (ICP-OES). All the experiments were carried out in triplicate.

### Statistical Design of Experiments

The statistical design to the boron remediation procedures was carried out. This provided less experimental time and cost, less number of experiments, and overall control of the experimental procedure in order to reach the preferred response. The statistical design defines individually the significance degrees of each experimental parameter and their interactions on the response; adsorption capacity is used as a response. In this project, various parameters and response (adsorption capacity) were examined by taking into accounts the regression model coefficients (Student's t test and P values (probability constants)). Boron analysis was performed in triplicates and the average of the results will be used in the statistical analysis.

## Chapter 4: RESULTS AND DISCUSSION

Characteristics of WTR, nano-WTR and its modified forms

FTIR characterization

Figure 14 shows the FTIR of untreated WTR and the average of 6 chemically modified WTR with different ratio of  $\text{HNO}_3/\text{H}_2\text{SO}_4$ . The FTIR peaks of the WTR are related to the polyisoprene vibrations; namely C=C-H stretching ( $3037\text{ cm}^{-1}$ ), CH symmetrical stretching ( $2915\text{ cm}^{-1}$ ), stretching of unsaturated double bond C=C ( $1536\text{ cm}^{-1}$ ),  $\text{CH}_2$  symmetrical stretching ( $2848\text{ cm}^{-1}$ ), and out-of-plane bending ( $818\text{ cm}^{-1}$ ), and deformation vibration of  $\text{CH}_2$  and  $\text{CH}_3$  ( $1432$  and  $1371\text{ cm}^{-1}$ ) in both WTR samples. The highest absorbance is in the wavelength of  $779\text{ cm}^{-1}$  for both samples which corresponded to the functional group (-C=C-H). The results agreed well with other studies such as (Datta & Wloch, 2015). Table 8 presented the main FTIR band of WTR. It was noticed that the main variations between the two spectra were in the region of  $1380$  and  $160\text{ cm}^{-1}$ . This confirmed the formation of new peaks as a results of acid reaction with the WTR. The peaks would help in enhancing the adsorption capacity of the WTR.

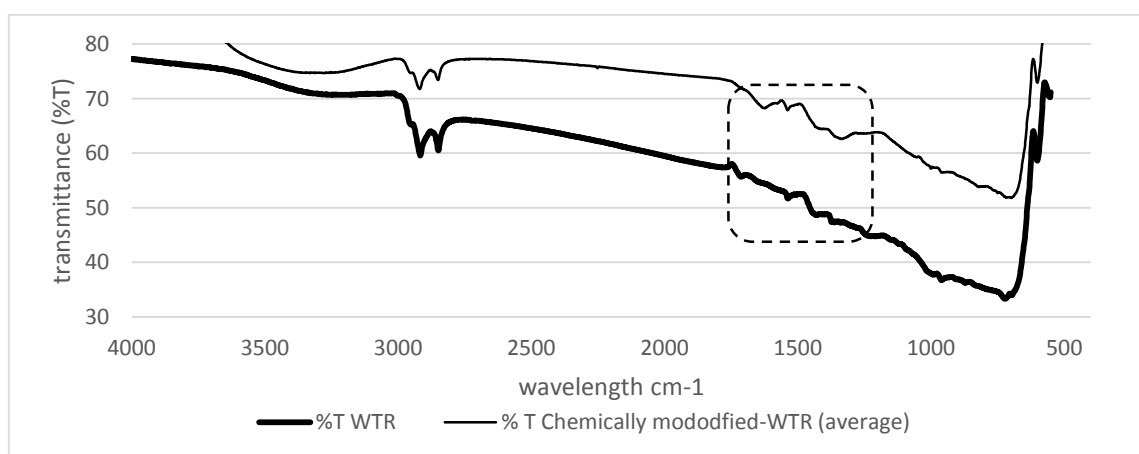


Figure 14: The FTIR spectra for WTR & Chemically modified WTR

Table 8 Most Significant Bands Of WTR(Colom Et Al. 2016).

Wavelength(cm <sup>-1</sup> )	Assignment	Component
1452	-CH <sub>2</sub> - stretching	R <sub>1</sub> R <sub>2</sub> C=CH <sub>2</sub>
1412	-C=C-H in plane C-H bend	R <sub>1</sub> R <sub>2</sub> C=CH <sub>2</sub>
1383	-CH <sub>3</sub> symmetric bend	
1096	Si-O stretching	SiO <sub>2</sub>
1021	-C-C- stretching	Black Carbon
874	-C=C-H in plane	R <sub>1</sub> R <sub>2</sub> C=CH <sub>2</sub>
716	-C=C-H in plane	R <sub>1</sub> R <sub>2</sub> C=CHR <sub>2</sub>
603	-C-S- stretching	
524	-S-S- stretching	
465	-S-S- stretching	

The SEM micrographs in the Figure 15 shows the surface morphology, particle size and homogeneity of different samples before and after the chemical and nano modification. All samples showed irregular shapes and sharp edges and that is mostly due to mechanical grinding of samples. The sample (A) shows particles more homogeneity than samples (B –G). The surface texture is less rough and smoother than other samples (Mousavi et al., 2010). The surface texture of the samples of chemical treatment (C-G) was rougher surface and more pores and edges than sample (A). It seems that the chemical treatment added surface area to the samples chemically treatment. The degree of roughness achieved with this treatment was related to the ability of the acid chemical treatment to degrade and remove partially some of the different components of the WTR inside or on the surface of the particle (Guo et al., 2013). Sample (B) is the nano-WTR sample, and it shows that it contain high amount of fibers with varying degree of length (approximate 0.1 – 600 μm) and diameters (approximate 5 -50 μm). It also shows smaller amount of WTR with sample length and diameter (approximate 0.5-100 μm). The fibers have pores along its axis.

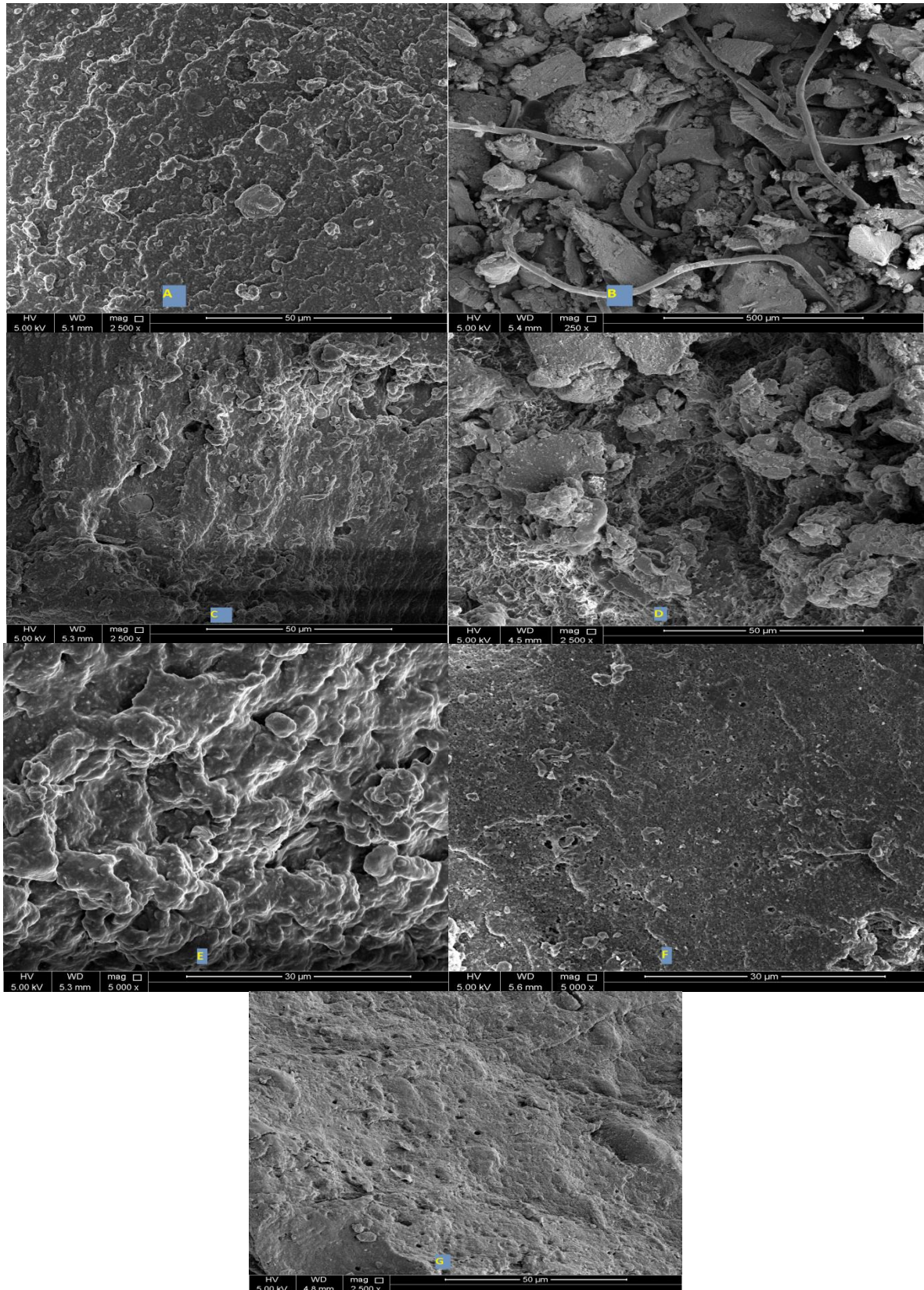


Figure 15: SEM micrograph of (a) WTR ,(b) NanoWTR ,(c) HNO<sub>3</sub> 1:3 H<sub>2</sub>SO<sub>4</sub> ,(d) H<sub>2</sub>SO<sub>4</sub> (e) HNO<sub>3</sub> 1:1 H<sub>2</sub>SO<sub>4</sub> ,(f) HNO<sub>3</sub>, (g) HNO<sub>3</sub> 3:1 H<sub>2</sub>SO<sub>4</sub>

Table (9) and Figure (16) show the results from using EDX elemental analysis of the WTR samples (chemically modified-WTR and Nano-WTR). The elemental measurement range was from C, O, Si, S, Ca, Na, Cl, Zn and N. These results indicate that weight % were mostly C (73%-90%) and O (4%-19%). The presence of Zn was due the nature of tire. Tire are made of vulcanized rubber; in which the vulcanization treatment converts natural rubber to more durable materials by adding accelerators such as sulfur and in the process zinc chloride to form polymer chains which give the tire more durability. Thus, when polymers bonds break, zinc and chloride released first (Ghosh et al., 2003). In the nano-WTR sample, the change in weight % in (O, S, and Zn), and addition of Na can be attributed to increase in fibers to WTR ratio, as presented in SEM microscopes.

The Ca is presumed to be contained as  $\text{CaCO}_3$ . This assumption was based on the fact that peaks (near  $1390\text{-}1450\text{ cm}^{-1}$  and  $760\text{-}850\text{ cm}^{-1}$ ) characteristic of  $\text{CaCO}_3$  in infrared spectra were also confirmed in the FTIR measurement results. The presence of Ca is also decreased in all chemical treatment, and that can be attributed to acid/base interactions, which formed salts, and in turn, removed by etching (submerging in D.W ) treatment prior to batch studies (Shimazu Corporation, 2016). The presence of Cl and N was found only in chemical treatment, which could be explained by exchange reactions with adsorbents ions. The chemical modified-WTR have in general lower adsorption curve compared to WTR, it most likely due to the weakening of the clustering and entanglement of long chains carbon particles. What bind the polymer together is the accelerators such as sulfur and zinc chloride, which help strengthening the bonds of polymers to form polymers chains. Thus, the chemical treatment, weaken those bonds, and lead to decrease in adsorption at FTIR (Gunasekaran et al., 2007). The CHN/O analysis for the WTR samples (chemically modified-WTR and nano-WTR) presented the following results: C: 84.58%, O: 3.61 % and H: 11.81 %; the results agreed with the finding in EDX analysis. The results were also agree with other elemental

analysis findings of untreated WTR from (Aisien et al., 2013; Cunliffe & Williams, 1998; Manchon Vizuite et al., 2004). Table (10) summarizes the CHN/O analysis carried out by other studies.

*Table 9: EDX Elemental Analysis -Wt.(%) of Element*

<b>Type of WTR</b>	<b>Wt.(%) of Element</b>								
	<b>C</b>	<b>O</b>	<b>Si</b>	<b>S</b>	<b>Ca</b>	<b>Na</b>	<b>Cl</b>	<b>Zn</b>	<b>N</b>
<b>No Treatment (WTR)</b>	88.2	4.83	0.34	3.11	0.57	0	0	2.95	0
<b>Nano-WTR</b>	85.09	10.51	0.29	1.57	0.66	0.69	0	1.59	0
<b>(ChemTr)HNO<sub>3</sub> 1:3 H<sub>2</sub>SO<sub>4</sub></b>	83.21	14.65	0	0.96	0.28	0	0.22	0	0
<b>(ChemTr)H<sub>2</sub>SO<sub>4</sub></b>	90.83	6.64	0	1.43	0.27	0.91	0	0.84	0
<b>(ChemTr)HNO<sub>3</sub> 1:1 H<sub>2</sub>SO<sub>4</sub></b>	75.64	18.16	0.14	0.14	0	0	0	0	4.56
<b>(ChemTr)HNO<sub>3</sub> 3:1 H<sub>2</sub>SO<sub>4</sub></b>	78.45	19.1	1.04	0	0.12	0	0.38	0	0
<b>(ChemTr)HNO<sub>3</sub></b>	73.53	19.28	0.12	1.88	0	0	0	0	5.19

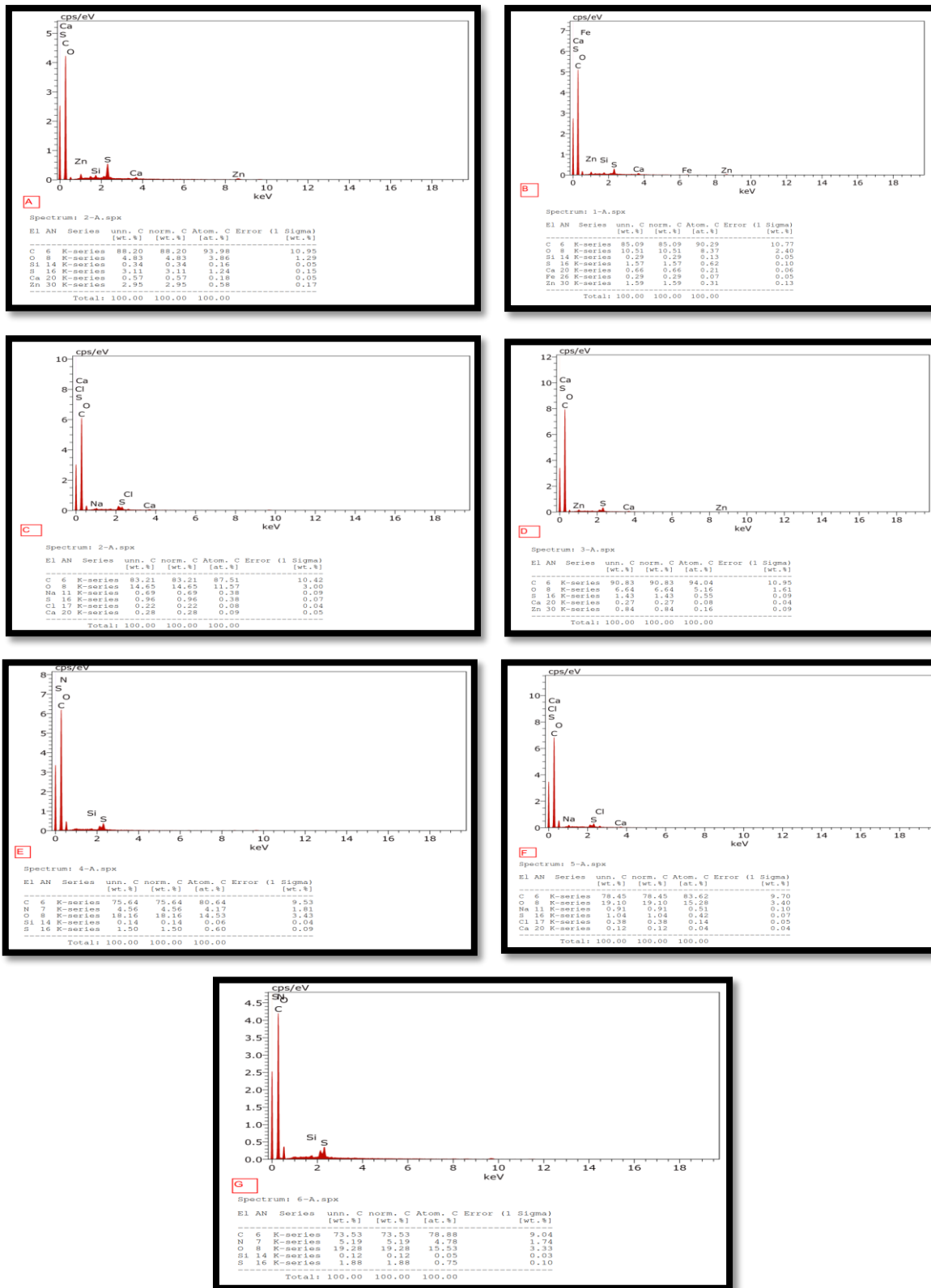


Figure 16: EDX Elemental Analysis of (a) WTR, (b) NanoWTR, (c) HNO<sub>3</sub> 1:3 H<sub>2</sub>SO<sub>4</sub>, (d) H<sub>2</sub>SO<sub>4</sub> (e) HNO<sub>3</sub> 1:1 H<sub>2</sub>SO<sub>4</sub>, (f) HNO<sub>3</sub>, (g) HNO<sub>3</sub> 3:1 H<sub>2</sub>SO<sub>4</sub>



Table 10: Characteristics Of WTR Compared To Other Studies

<b>Characteristics</b>	<b><i>This study</i></b> <b><i>(untreated</i></b> <b><i>WTR)</i></b>	<b><i>Amenaghawon</i></b> <b><i>et al. (2013)</i></b>	<b><i>Cunliffe</i></b> <b><i>and</i></b> <b><i>Williams</i></b> <b><i>(1998)</i></b>	<b><i>Gonzalez</i></b> <b><i>e et al.</i></b> <b><i>(2001)</i></b>	<b><i>STD</i></b>
<b>Carbon</b>	88.2	86.5	86.4	86.7	0.4213
<b>Hydrogen</b>	11.81	6.64	8	8.1	1.1086
<b>Oxygen</b>	3.61	1.1	3.4	1.3	0.6680
<b>Nitrogen</b>	0	0.4	0.5	0.4	0.1108
<b>Sulfur</b>	3.11	2	1.7	1.4	0.3731

Boron adsorption by WTR

pH effect on Boron adsorption by WTR

Figure 17 shows the effect of pH on the adsorption of boron on WTR. After the statistical analysis, it was concluded that there was a significance difference between the means of samples at 95% confidence level. Furthermore, using Tukey test to find and categorize means that were significantly different from each other. Following that, the highest adsorption of boron was at pH 2 at the value of  $8.45 \pm 0.01$  mg/g. The remaining pH values have no significance difference between each other. The adsorption capacities at different pH values were pretty constant. Therefore, for the following parameters (for WTR & Nano-WTR) which are the initial concentration, particles size, adsorbent dosage, the optimum pH value would be 4 to ensure highest adsorption efficiency. This was explained in the previous chapter; which the boron adsorption follows the boron speciation (Schott et al., 2014).

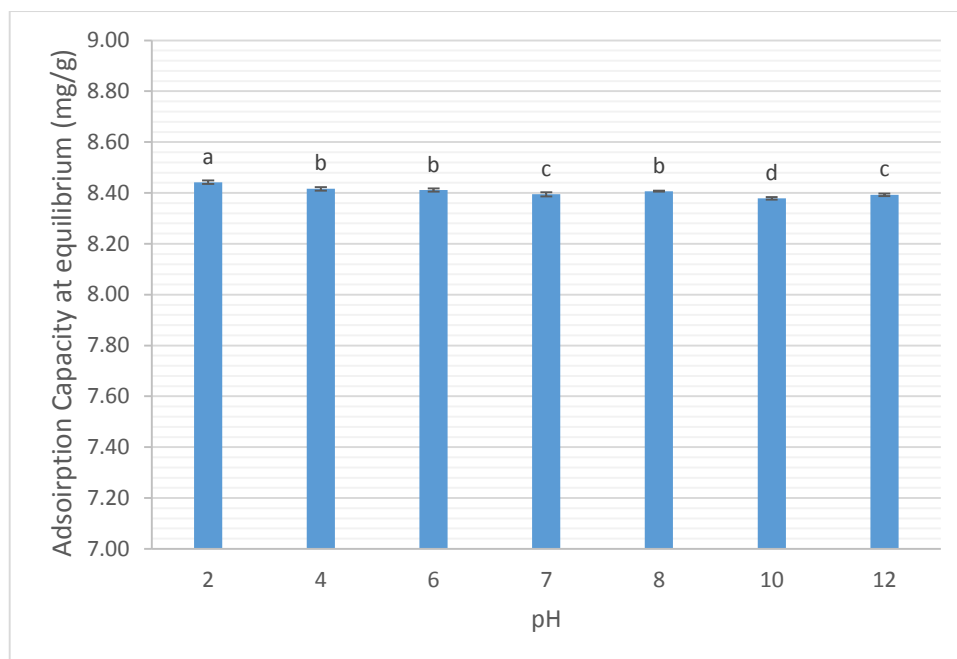


Figure 17: pH Effect on the adsorption of Boron on WTR

Operational settings: Adsorbate mass : 0.05 g, Solution volume :50 mL, Contact time : 48 h, Temperature : 294.45 K , Rotation speed: 150 rpm , pH : 2 , 4, 6, 7, 8, 10, 12.

#### Adsorbent dosage effect on Boron adsorption by WTR

Figure 18 illustrates the effect of adsorbent mass in the WTR adsorption capacity. The adsorption capacity can be observed to be decreased with increase in dosage of adsorbent; signifying that the dose of adsorbent have an effect on the process of adsorption. After ANOVA statistical analysis, it was concluded that there is significance difference between means of samples at 95% confidence level. Furthermore, using Tukey test to find and categorize means that are significantly different from each other. Following that, the highest adsorption of boron was at dosage of 0.05 g of adsorbent at the value of  $5.32 \pm 0.01$  mg/g.

In the literature, the adsorption capacity is usually increased as adsorbent dosage increases. According to study by Namasivayam & Kavitha, 2002, the study showed linear positive correlation between removal percentage of “Congo red” vs. adsorbent dosage which is “coir pitch carbon” ; the removal percentage were 18%, 78%, 90% and 98% removal of adsorbate

Congo red , at 100, 400, 700 and 900 mg of adsorbent coir pitch carbon , respectively. In another study carried out by Sivaraj et al., 2001, showed a linear positive correlation between removal % of “Acid dye” versus adsorbent dosage which is “peel of waste orange”; the removal percentage were 60%, 80% and 99% removal of adsorbate Acid dye, at 200, 400 and 600 mg of adsorbent peel of waste orange , respectively.

The above trend could be explained by Mittal et al., (2010). This is likely due to most of the boron were already adsorbed when the dosage is high. Another cause, is when calculating the adsorption capacity, the difference between initial concentration and equilibrium concentration is divided by the mass of adsorbent; thus the ratio of increase in adsorption capacity should be equal or more than mass of adsorbent to present the positive slope between adsorption capacity at equilibrium vs. adsorbent dosage. The solution is to adjust the trend of the result, is to increase the initial concentration of boron to 200 mg/L instead of 50 mg/L.

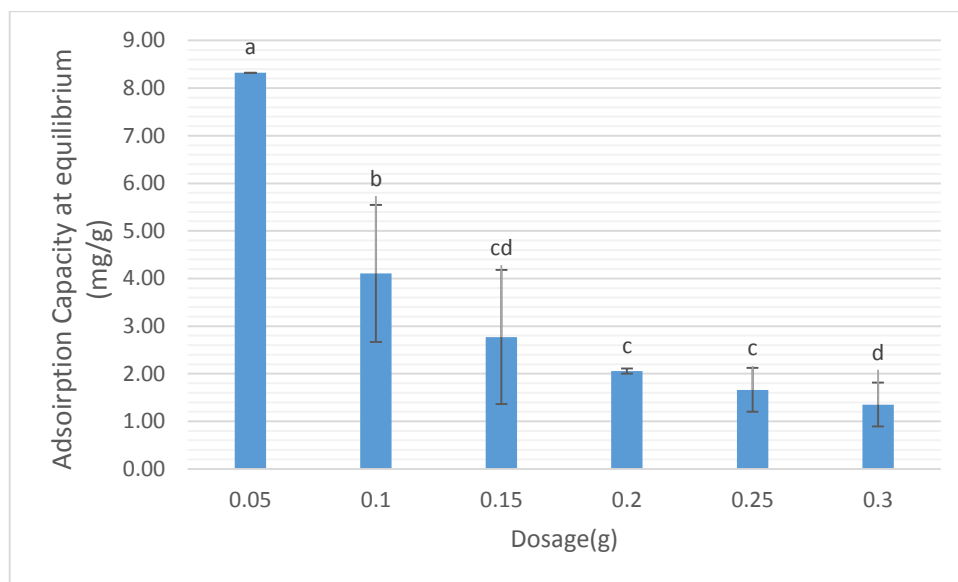


Figure 18: Dosage of adsorbent effect on Boron adsorption.

Operational settings: Adsorbate mass : 0.05 g, 0.1 g, 0.15 g, 0.2 g, 0.25 g, 0.3 g, Solution volume: 50 mL, Contact time : 48 h, Temperature : 294.45 K , speed: 150 rpm , pH : 2

Adsorbent particle size effect on Boron adsorption.

Figure 19 shows the effect of particles size on the adsorption capacity. The figure indicates that as the particle size of adsorbent increases, adsorption capacity of boron decreases. Except in the case of 0.06-125  $\mu\text{m}$ , which is explained by ratio of fibers to WTR particles. The increase of fibers and decrease in WTR particles in the nano-WTR led to decrease in the adsorption capacity, due to WTR having higher adsorption capacity. After the ANOVA statistical analysis, it was concluded that there is no significant difference between means of samples at 95% confidence level. Furthermore, using Tukey test to find and categorize means that are significantly different from each other. Which indicated that the particles size (125-250, 250-500 and 500-1000  $\mu\text{m}$ ) had no significant difference. Therefore, the highest adsorption of Boron was recorded at  $8.32 \pm 0.00$  mg/g for particle size of in the range of 125-500  $\mu\text{m}$ .

In the literature, the adsorption capacity versus adsorbent size has always a negative linear correlation. According to study investigated by Engates & Shipley,(2011) the adsorption of three heavy metals ( $\text{Pb}^{+2}$ ,  $\text{Cd}^{+2}$  and  $\text{Ni}^{+2}$ ) onto two TiO adsorbent (Nano & Bulk) showed that the maximum adsorption capacity at equilibrium  $Q_m$ ; 401.1, 135.1, 114.9  $\mu\text{g/g}$  for Nano- TiO for  $\text{Pb}^{+2}$ ,  $\text{Cd}^{+2}$  and  $\text{Ni}^{+2}$ , respectively; and 312.4, 55.4, 63.8  $\mu\text{g/g}$  for Bulk- TiO for  $\text{Pb}^{+2}$ ,  $\text{Cd}^{+2}$  and  $\text{Ni}^{+2}$ , respectively. The study indicated that the  $Q_m$  for Nanoparticles was higher than the bulk.

Krishna & Swamy., (2012) investigated the effect of particle size of calcined brick powder for the adsorption of  $\text{Cr}^{+4}$ . The study showed that the amounts adsorbed for 1.7, 0.8 and 0.6 mm particle size were 2.34, 2.66 and 3.01 mg/g, respectively. The study indicated the negative correlation with adsorption capacity versus increase in particle size.

According to Aisien et al., (2013), the above observation can be clarified by the statement that the greater of the interior surface area and volume of micro-pores, the smaller of the size of the adsorbent particles. Thus, more active sites are adsorption accessible to bind. Nonetheless, for adsorbent with larger particle size, the ratio of diffusion resistance in pores to mass of transfer is higher; therefore, most of adsorbent internal surfaces may not be exploited for adsorption and subsequently, the amount of Boron adsorbed is small.

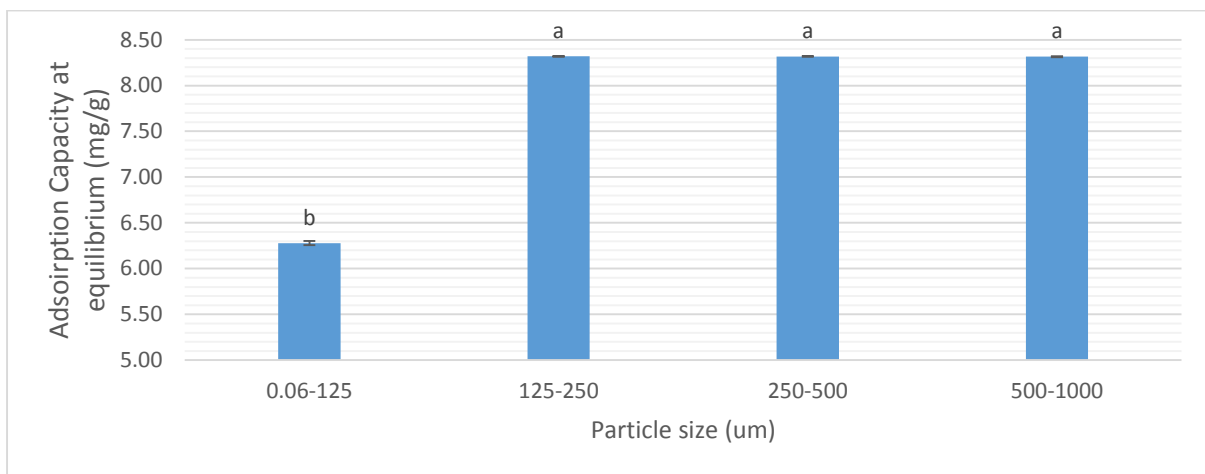


Figure 19: Particle size effect on boron adsorption.

Operational settings: Adsorbate mass : 0.05 g, Solution volume :50 ml, Contact time : 48 h, Temperature : 294.45 K , Rotation speed: 150 rpm , pH : 2.

#### Initial Concentration effect on the adsorption of Boron on WTR

Figure 20 presented the effect of initial boron concentration on the WTR adsorption capacity. After ANOVA statistical analysis, it was concluded that there is significance difference between means of samples at 95% confidence level. Furthermore, using Tukey test to find and categorize means that are significantly different from each other, it was found that the following initial concentration yield the highest adsorption capacity: 17.5 mg/L. The development detected signifies that as the initial concentration increases, equilibrium

concentration of boron increases. The trend will continue till it reaches point where it will be constant onward. The highest adsorption capacity was observed at  $16.72 \pm 0.00$  mg/g for initial concentration of 17.5 mg/L.

According to Mittal et al., (2010), the trend can be explained as the following: the increase in the adsorption capacity could be due to greater interaction between boron and WTR. This will enhance the boron diffusion and decreased the resistance to uptake. However, increasing the boron concentration above 15.7 mg/l causes a little increase in the amount of boron adsorbed; indicating near saturation of the adsorption sites.

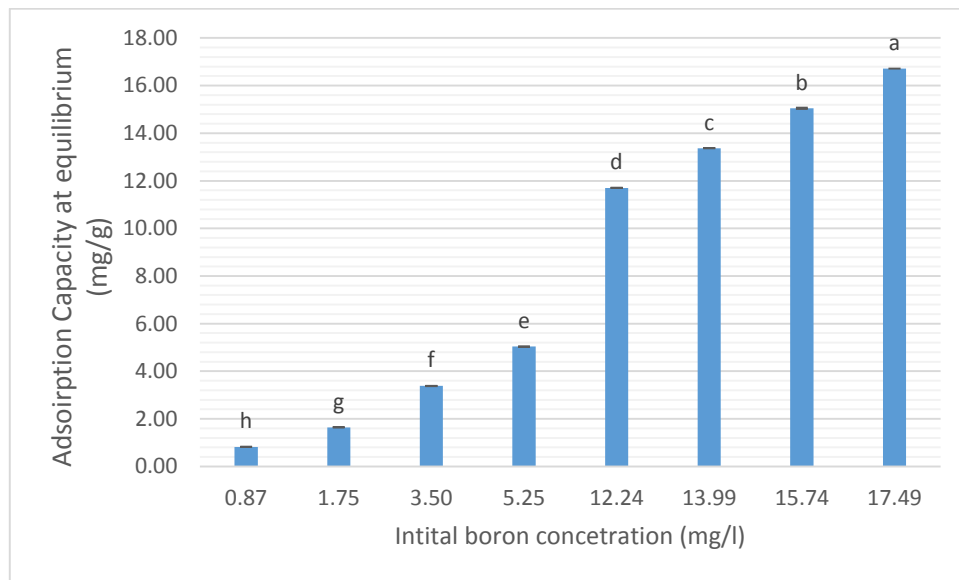


Figure 20: Initial Concentration effect on the adsorption of Boron on WTR

Operational settings: Adsorbate mass : 0.05 g, Solution volume :50 ml, Contact time : 48 h, Temperature : 294.45 K , Rotation speed: 150 rpm , pH : 2. Boric acid concentration was 50 mg/L = 17.49 mg Boron/L

## Boron adsorption by chemically modified WTR

### pH effect on Boron adsorption by chemically modified WTR

Figure 21 shows the effect of pH on the adsorption of boron on chemically modified WTR. After the ANOVA statistical analysis, it was concluded that there is significance difference between means of samples at 95% confidence level. Furthermore, using Tukey test to find and categorize means that are significantly different from each other, it was found that the following 17 interactions of pH & ratio yield the highest adsorption capacity (pH, ratio): (2, HNO<sub>3</sub>), (4, HNO<sub>3</sub> 3:1 H<sub>2</sub>SO<sub>4</sub>), (2, 4), (8, H<sub>2</sub>SO<sub>4</sub>), (7, H<sub>2</sub>SO<sub>4</sub>), (8, HNO<sub>3</sub> 3:1 H<sub>2</sub>SO<sub>4</sub>), (2, H<sub>2</sub>SO<sub>4</sub>), (7, HNO<sub>3</sub> 1:1 H<sub>2</sub>SO<sub>4</sub>), (3, H<sub>2</sub>SO<sub>4</sub>), etc. The highest adsorption capacity was at  $8.41 \pm 0.00$  mg/g for (pH 2, HNO<sub>3</sub> 1:3 H<sub>2</sub>SO<sub>4</sub>).

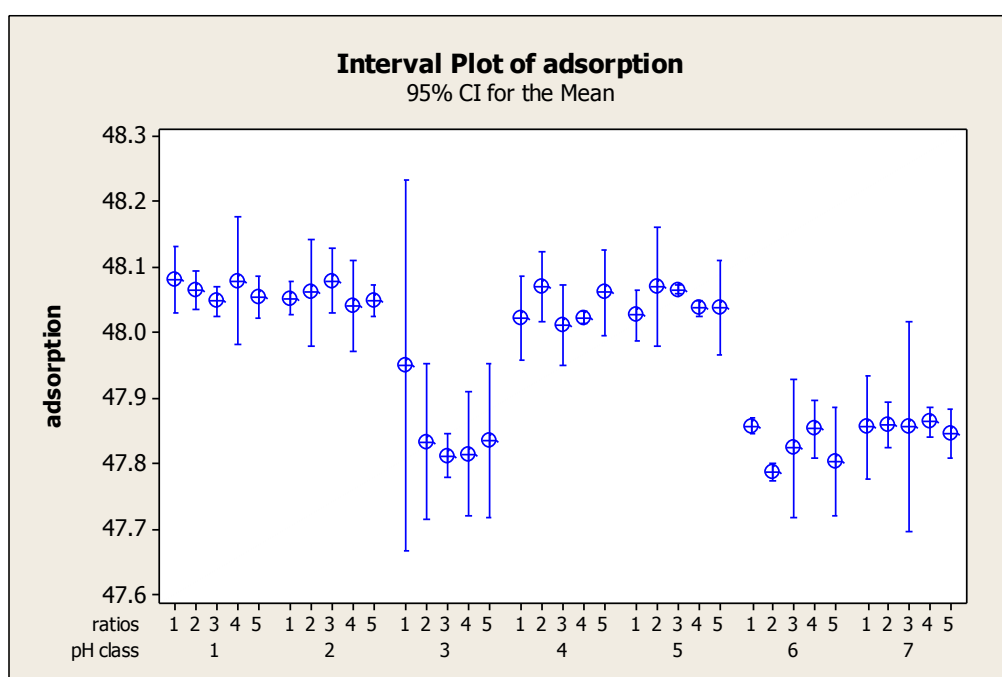


Figure 21: pH effect on the adsorption of Boron on chemically modified WTR. Where ratio 1: HNO<sub>3</sub> , ratio 2:H<sub>2</sub>SO<sub>4</sub> , ratio 3: HNO<sub>3</sub> 3:1 H<sub>2</sub>SO<sub>4</sub> , ratio 4: HNO<sub>3</sub> 1:3 H<sub>2</sub>SO<sub>4</sub> and ratio 5: HNO<sub>3</sub> 1:1 H<sub>2</sub>SO<sub>4</sub> ; And Where pH class 1: pH 2 , pH class 2: pH 4, pH class 3: pH 6, pH class 4: pH 7, pH class 5: pH 8, pH class 6: pH 10, pH class 7: pH 12

### Initial Concentration effect on Boron adsorption by chemically modified WTR

Figure 22 presented the initial concentration effect on the adsorption of Boron on chemically modified WTR. After the ANOVA statistical analysis, it was concluded that there is significance difference between means of samples at 95% confidence level. Furthermore, using Tukey test to find and categorize means that are significantly different from each other, it was found that the following initial concentration yield the highest adsorption capacity: (17.5 mg/L). The highest adsorption capacity was  $13.81 \text{ g} \pm 0.02 \text{ mg/g}$  for initial concentration of 17.5 mg/L. The above explanation would be also valid here [This will enhance the boron diffusion and decreased the resistance to uptake].

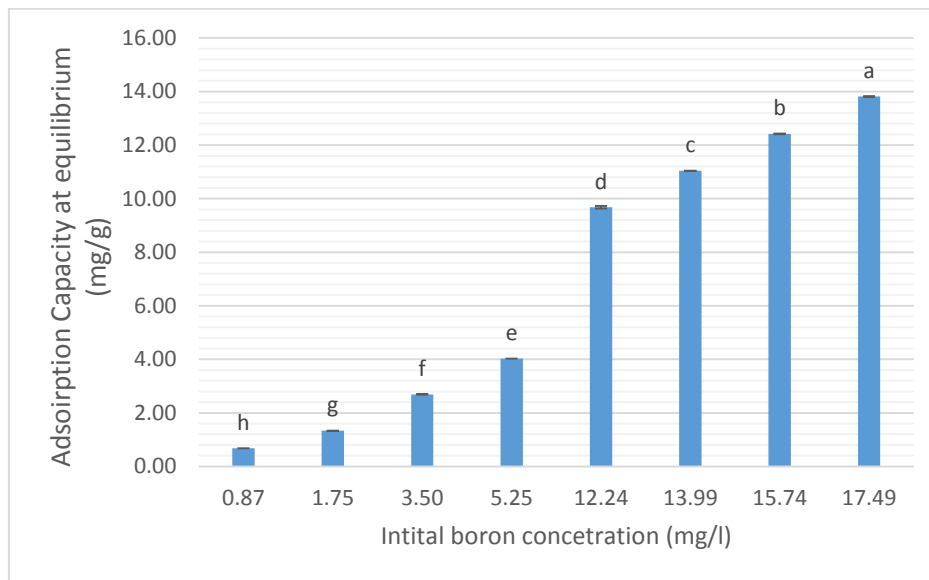


Figure 22: Initial concentration effect on the boron adsorption on chemically modified WTR

Operational settings: Adsorbate mass : 0.05 g, Solution volume :50 ml, Contact time : 48 h, Temperature : 294.45 K , speed: 150 rpm , pH : 2. Boric acid concentration was 50 mg/L = 17.49 mg Boron/L



## Boron adsorption by Nano-WTR

### Initial Concentration effect on Boron adsorption by Nano-WTR

Figure 23 shows the initial concentration effect on the adsorption of Boron on Nano-WTR. After the ANOVA statistical analysis, it was concluded that there is significance difference between means of samples at 95% confidence level. Furthermore, using Tukey test to find and categorize means that are significantly different from each other, it was found that the following initial concentration yield the highest adsorption capacity: (13.9, 15.7 and 17.5 mg/l). The highest adsorption capacity is  $12.7 \pm 1.78$  mg/g for initial concentration of 17.5 mg/L.

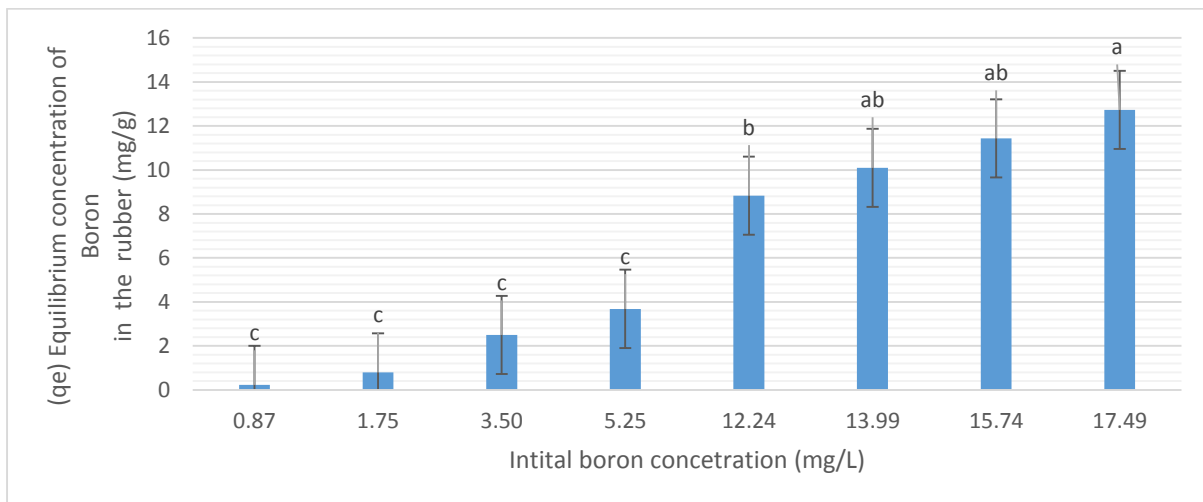


Figure 23: Initial Concentration effect on the adsorption of Boron on Nano-WTR

Operational settings: Adsorbate mass : 0.05 g, Solution volume :50 ml, Contact time : 48 h, Temperature : 294.45 K , Rotation speed: 150 rpm , pH : 2. Boric acid concentration was 50 mg/L = 17.49 mg Boron/L

## Leachability of WTR

Figure 24 shows that the highest leachability was for Zn in the amount of 1635  $\mu\text{g/L}$  from WTR. This trend is quite logical since the Zn make up almost 2 % weight of WTR according to Elemental analysis using EDX. The trend followed by Fe (179.45  $\mu\text{g/L}$ ), Pb

(117.41  $\mu\text{g/L}$ ), Cd (6.83  $\mu\text{g/L}$ ) and Cr 0.44  $\mu\text{g/L}$ ). The Zn had the highest leachability was due to having an average of 4.5 weight % of WTR. The reason of high weight % of Zn is due the nature of tire. Tires are made of vulcanized rubber in which the vulcanization treatment converts natural rubber to more durable materials by adding accelerators such as sulfur and in the process they use zinc chloride to form polymer chains which give the tire more durability. Thus, when polymers bonds break, zinc and chloride released first (Ghosh et al., 2003). According to Gleadthorpe, 2008, the maximum permissible concentration in soil for Zn, Cd, Pb and Cr were 225 mg/kg , 3 mg/kg, 300 mg/kg and 400 mg/kg of soil. No health-based guideline value for iron is proposed according to World health Organization (WHO). Therefore, Zn, Cd, Pb and Cr concentration in this study are less than 1000 times from the maximum permissible concentration. However, it may have the potential to accumulate over time with the large quantity of tire waste. It also observed that increase in pH lead to decrease in Leachability of Fe, Pb and Zn.

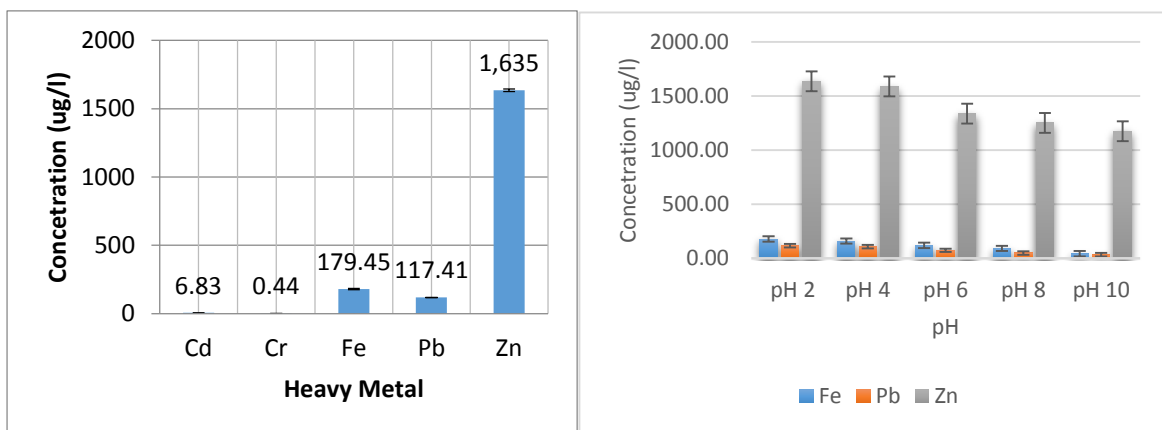


Figure 24: Heavy Metals Leachability from WTR.

Operational settings: Adsorbate mass : 1 g, Solution volume :50 ml, Contact time : 24 h, Temperature : 294.45 K , Rotation speed: 150 rpm , pH : 2, 4, 6, 8, 10.

## Isotherm Models

In equilibrium, a relationship exists between the boron concentration in the solution and amount of boron adsorbed. The relationship is defined as adsorption isotherms, which is generally a ratio of quantity adsorbed by the adsorbent and quantity remained in the solution at equilibrium under fixed temperature conditions. To study the connection between boron uptake ( $Q_e$ ) and the equilibrium concentration in the solution ( $C_e$ ), adsorption isotherm models are generally applied for fitting the experimental data. Two isotherm models were investigated namely the Freundlich isotherm and Langmuir models. The curves of the related adsorption isotherms are regressed and parameters of the equation are thus obtained (Aisien et al., 2013).

### Langmuir and Freundlich Adsorption Isotherm

Figures 25 and 26 show the linearized Langmuir and Freundlich isotherm models for the WTR, chemical modified WTR, and nano-WTR. The parameters of the Langmuir isotherm model are shown in Table 11. In Freundlich isotherm model, the slope ( $n$ ) ranges between (0 – 1) and is a measure of surface heterogeneity, becoming more heterogeneous as its value gets closer to zero. From Table 11, it was found that all  $n$  value are in the range of (1.054 - 1.95); indicating high heterogeneity. The values of the Freundlich and Langmuir isotherms parameters as well as the correlation coefficient ( $R^2$ ) of the adsorption of boron by WTR are given in Table 11. In Table 11, the isotherms experiments signify that the adsorption of boron was best fitted by the Freundlich isotherm model for all type of treatment of WTR as indicated by the higher  $R^2$  value achieved for the Freundlich isotherm compared to Langmuir model. It also evident by the lower SSE value, which indicate better fit for the model. This suggests that the adsorption of Boron by WTR, Chemically modified-WTR and

Nano-WTR is in a heterogeneous surface. It also indicates that Boron was adsorbed as multilayers on the adsorbate surface. It was also noticed that the Langmuir adsorption capacities were in negative values; indicating the non-applicability of the model. Langmuir isotherm, in its derivation form indicates a homogeneous adsorption, in which all sites retain equivalent attraction for the adsorbate. This would confirm that the surfaces of the adsorbents are not homogeneous. This totally agrees with the Freundlich isotherm model, in which the  $R^2$  were high for all the adsorbents.

It can also be concluded that the fitting results indicate that the Freundlich model fits the experimental data much better than the Langmuir model. Correlation coefficient factors ( $R^2$ ) for Freundlich models are around 0.88 - 0.99. The fitness of the Freundlich isotherm model in the present study can be elucidated by the surface precipitation model, which describes both the precipitation reaction and the adsorption reaction at the adsorbent surface. This model describes multilayer adsorption processes, resulting in higher boron concentrations (Aisien et al., 2013; Mittal et al., 2010; Namasivayam & Kavitha, 2002).

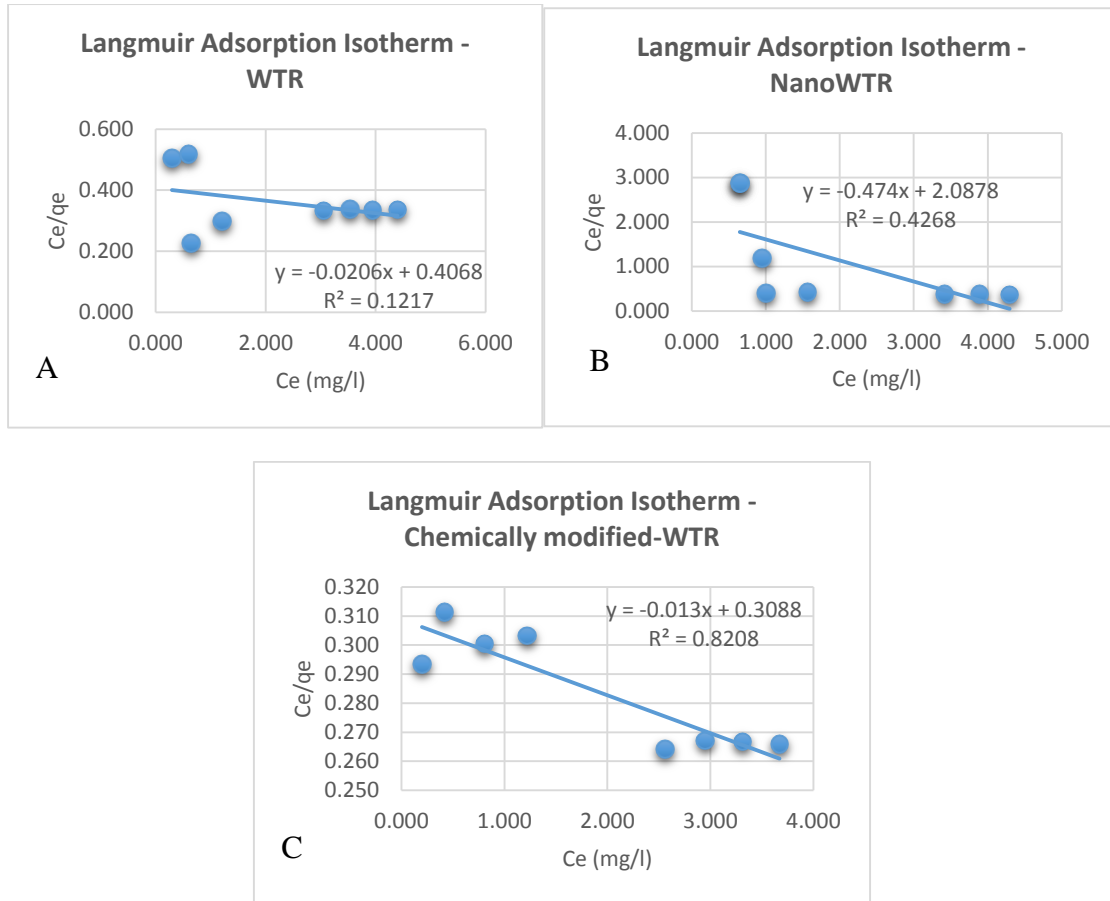


Figure 25: Linearized Langmuir Adsorption Isotherms plotted for batch adsorption experiment, Where A: WTR, B: Nano-WTR and C: Chemically Modified WTR.

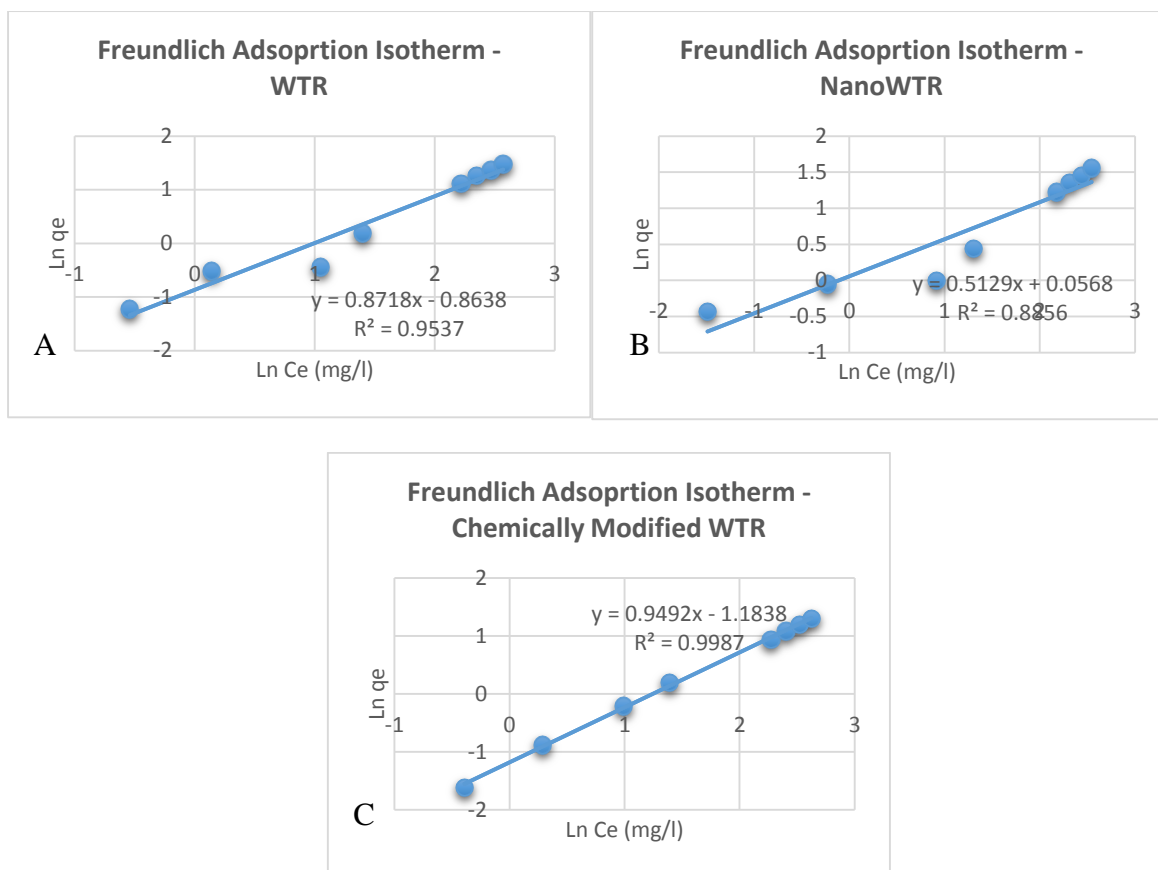


Figure 26: Freundlich Adsorption Isotherms plotted for batch adsorption experiment, Where A: WTR, B: Nano-WTR and C: Chemically Modified WTR.

Table 11 Parameters For Langmuir And Freundlich Isotherms

Parameters	Freundlich isotherm				Langmuir isotherm			
	Kf (mg/g)	R <sup>2</sup>	n	SSE	Q° (mg/g)	R <sup>2</sup>	b (L/mg)	SSE
WTR	2.37	0.9537	1.147	34.1	-48.544	0.1217	2.458	441.9
Nano-WTR	1.058	0.8856	1.95	41.7	-2.11	0.4268	2.0878	67.1
Chemically modified WTR	3.267	0.9987	1.054	47.1	-76.923	0.8208	3.238	671.1

Table 12 presents the contribution of different authors on the use of WTR in various pollutants' removal. Table 12 shows the adsorption capacity at equilibrium of adsorbent derivate from WTR, either by chemical treatment or no treatment. The highest adsorption capacity was observed at the adsorbent AC-4 for heavy metals, at 3.15-14.6 mg/g; followed by adsorption capacity from this study in the adsorption of boron highest at chemically modified-WTR, and lowest at Nano-WTR, at 3.27 mg/g and 1.16 mg/g, respectively. According to Nieto-Márquez, et al., 2017, the high adsorption capacity at equilibrium of AC is due to having high affinity (N) of adsorbent (AC) to adsorbate  $Pb^{+2}$ ,  $Cd^{+2}$  and  $Cr^{+3}$  and also due to exchange/sharing of electrons.

*Table 12 Comparison of This Study with Other on Freundlich Isotherm on the Use of WTR as Adsorbent*

References		Freundlich Isotherm			
This Study	Parameters	$K_f$ (mg/g)	$R^2$	N	
	WTR	2.37	0.9537	1.147	
	Nano-WTR	1.058	0.8856	1.95	
	Chemically Modified WTR	3.267	0.9987	1.054	
(Aisien et al., 2013)	WTRG For Ethylbenzene	3.168	0.706	3.759	
(Nieto-Márquez, et al., 2017)	Activated	$Pb^{2+}$	14.62	0.9672	3.55
	Carbon(AC- 4)	$Cd^{2+}$	3.15	0.8791	3.54
		$Cr^{3+}$	14.40	0.8648	6.65
(Imyim et al., 2016)	Cationic	As(III)	0.0131	0.9134	0.3569
	Polymer- Modified WTR	As(V)	0.1806	0.984	0.7581

## Kinetics of adsorption

In most kinetic adsorption models, empirical equations are used to describe the concentration of various pollutant in aqueous solution as a function of time. These include: Lagergren pseudo-first order model, pseudo-second order model, and Elovich models. Figure 27 presents the kinetic study of the boron removal from the WTR. It shows a rapid increase in removal % of boron in the 1<sup>st</sup> 65 minutes in the case of 1 g dosage, and followed by a slow decrease in removal % till 120 minutes. The highest removal % was observed in 65 minutes at value of 76.7%. Figure 28 also shows a rapid increase of removal % till 30 minutes, followed by a slower increase till 65 minutes in the case of 1.5 g dosage. The highest removal % was observed in 65 minutes at value of 75.7 %. After that, it shows a slow decrease in removal % till 120 minutes.

The kinetic profile signifies that the adsorbent was saturated, and the equilibrium was reached after 65 min. This could be explained by Aisien et al., 2013 in which all available active binding sites were unavailable due to their occupying by the boron molecules. In addition, some boron desorption may take place concurrently with the adsorption development. Thus, no evident increase in adsorption of boron was observed. It may also be concluded that the adsorption equilibrium indicated a fast boron adsorption by the WTR at both dosages. This kinetic development detected at the early phase can be credited to the surplus accessibility of binding active sites as it progresses; causing the incapability of the WTR to eliminate boron at late stage (Farouq & Yousef, 2014; El-Sherif et al., 2013; Ghasemi et al., 2013; Yüksel and Yürüm, 2009).



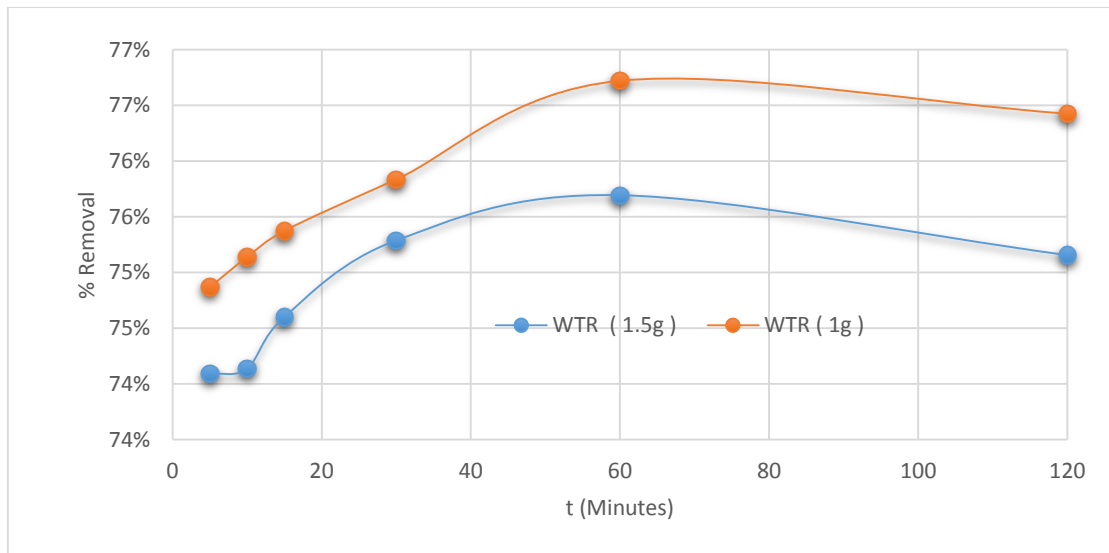


Figure 27: Boron removal percentage as function of time for 2 WTR dosage (1g and 1.5 g).

Operational settings: Adsorbate mass : 1 g & 1.5 g, Solution volume :1700 ml, Contact time : 2 h, Temperature : 294.45 K , Rotation speed: 150 rpm , pH : 2.

By plotting  $\ln(Q_e - Q_t)$  versus  $t$ , the slope will be  $\ln(Q_e)$  and the Intercept will be  $-k_1$ . Table 13 presents the linearized pseudo first order kinetic model. The  $Q_e$  and  $K_1$  were 0.28 and 0.004 for 1.5 g WTR and 0.59 and 0.01 for 1 g WTR, respectively. The correlation coefficients ( $R^2$ ) values were 0.04 for 1.5 g WTR & 0.66 for 1.5 g WTR. It was noticed that the theoretical  $Q_e$  did not equal the experimental  $Q_e$  for 1.5 g for both dosages. Therefore, it could be concluded that the Lagergren Pseudo first order model does not fit with the experimental data (El-Sherif et al., 2013; Ghasemi et al., 2013).

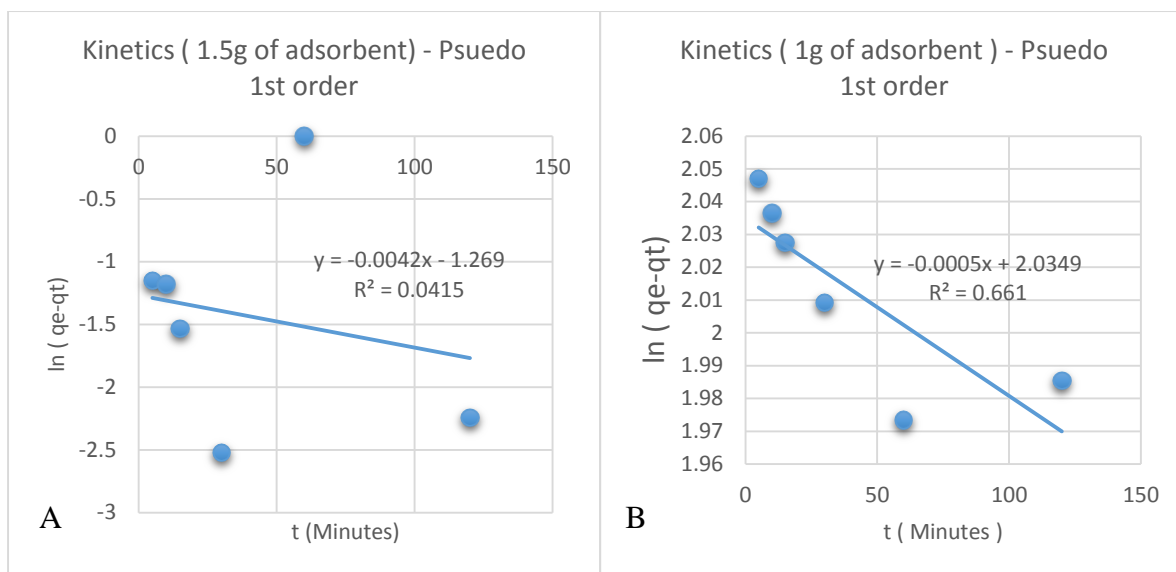
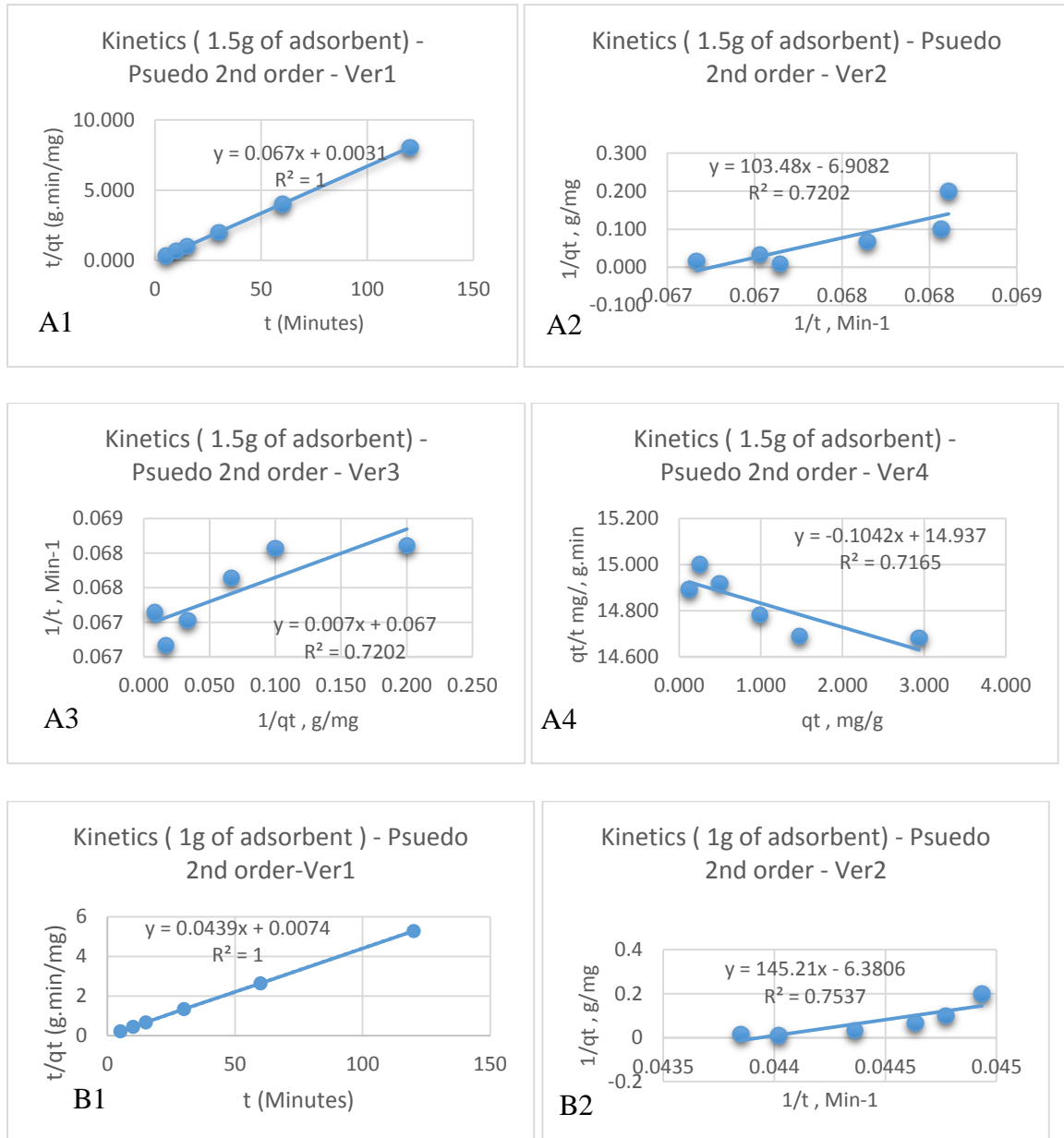


Figure 28 Lagergren Pseudo first order kinetic model plotted for adsorption study of WTR; where A: for 1.5g WTR, B: 1 g WTR ; Operational settings: Adsorbate mass : 1 g, Solution volume :1700 ml, Contact time : minutes, Temperature : 294.45 K , Rotation speed: 150 rpm , pH : 2.

In order to calculate the pseudo-second order (PSO) kinetic models, different modified models were investigated; namely PSO-model version 1 ( $t/q_t$  vs.  $t$ ), version 2 ( $1/q_t$  vs.  $1/t$ ), version 3 ( $1/t$  vs.  $1/q_t$ ) and version 4 ( $q_t/t$  vs.  $q_t$ ). Figure 29 and Table 14 show the calculated pseudo-second order adsorption capacity (mg/g) & rate constant  $K_2$  ( $g\ mg^{-1}\ min^{-1}$ ) using the above modified models. PSO-model version 1 presented the best fit, in term of value of correlation ( $R^2$ ) and in term of variation between experimental and calculated  $q_e$ . Therefore, it could be concluded that it is not advised to apply version 2, 3 and 4 the others version are not highly recommended, and the 1<sup>st</sup> version was the best PSO-model representative model for both 1 and 1.5 g WTR (Ghasemi et al., 2013). The value for PS-model-Ver1 rate constant  $K_2$  for 1 g and 1.5 g WTR were  $0.74\ g\ mg^{-1}\ min^{-1}$  and  $1.45\ g\ mg^{-1}\ min^{-1}$ , receptively. The decrease in PSO-model rate constant  $K_2$  value from 1 g to 1.5 g was doubled. The value for PSO-model-Ver1 calculated adsorption capacity ( $q_e$ ) for 1 g and 1.5 g WTR was 22.78 mg/g and 14.93 mg/g, receptively. The decrease in the PSO-model Ver1 calculated adsorption

capacity ( $q_e$ ) value from 1 g to 1.5 g WTR was almost doubled. The value of  $R^2$  for both 1.5 g and 1g WTR were excellent;  $R^2 = 1$ .



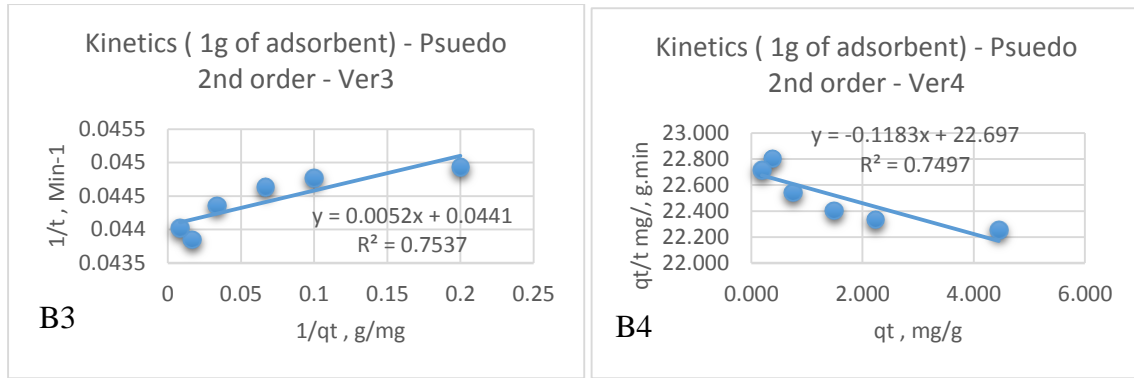


Figure 29 Pseudo second order kinetic model plotted for adsorption study of WTR; where A: for 1.5g WTR, B: 1 g WTR, and 1-4: Pseudo-second order Linearized version number

Operational settings: Adsorbate mass : 1 g, Solution volume :1700 ml, Contact time : minutes, Temperature : 294.45 K , Rotation speed: 150 rpm , pH : 2.

Figure 30 and Table 13 present the Elovich model parameters. By plotting  $qt$  versus  $\ln t$ , the  $\beta$  (1/slope) and the intercept of  $\alpha$  (exponent((intercept $\cdot\beta$ )- $\ln \beta$ )) can be obtained. These are: 10.63 g/mg and  $1.1 \times 10^6$  mg/g min for 1.5 g WTR, and 5.7 g/mg and  $4.4 \times 10^5$  mg/g min for 1 g WTR , respectively. The  $R^2$  values were 0.73 for 1.5 g WTR and 0.85 for 1.5 g WTR.

Table 13 Parameter Values For Pseudo First Order, Pseudo Second Order and Elovich Models

<b>Pseudo First-Order</b>					
<b>Parameters</b>	<b><math>k_1</math> (<math>\text{min}^{-1}</math>)</b>	<b>qe Calculated (mg/g)</b>	<b><math>R^2</math></b>	<b>qe Experimental (mg/g)</b>	<b>Average relative error deviation(ARED)</b>
<b>WT 1 g</b>	0.004	0.59	0.40	22.8	97.38
<b>WTR1.5 g</b>	0.012	0.28	0.04	15	98.11
<b>Pseudo Second-Order- Version 1</b>					
<b>Parameters</b>	<b><math>k^2</math> (<math>\text{gmg}^{-1}\text{min}^{-1}</math>)</b>	<b>qe Calculated (mg/g)</b>	<b><math>R^2</math></b>	<b>qe Experimental (mg/g)</b>	<b>Average relative error deviation(ARED)</b>
<b>WT 1 g</b>	0.74	22.78	<u>1</u>	22.8	<u>0.69</u>
<b>WT 1.5 g</b>	1.48	14.93	<u>1</u>	15	<u>1.21</u>
<b>Elovich Model</b>					
<b>Parameters</b>	<b><math>\alpha</math> (<math>\text{gmg}^{-1}\text{min}^{-1}</math>)</b>	<b><math>\beta</math> Calculated (g/mg)</b>	<b><math>R^2</math></b>	<b>qe Experimental (mg/g)</b>	<b>Average relative error deviation(ARED)</b>
<b>WT 1 g</b>	$4.4 \times 10^{53}$	10.63	0.90	22.8	28.31
<b>WT 1.5 g</b>	$1.1 \times 10^{66}$	5.7	0.73	15	74.48

Table 14: List Of Parameters For Pseudo-Second Kinetic Model For The Boron Adsorption Onto WTR

Parameter	q <sub>e</sub> calculated (mg/g)	K <sub>2</sub> (g mg <sup>-1</sup> min <sup>-1</sup> ) 1)	R <sup>2</sup>	q <sub>e</sub> experimental (mg/g)
<b>1.5 g WTR – Model Ver1</b>	<u>14.93</u>	<u>1.448</u>	<u>1</u>	<u>15</u>
<b>1.5 g WTR– Model Ver2</b>	-0.14	0.461	0.72	15
<b>1.5 g WTR– Model Ver3</b>	-0.10	0.641	0.72	15
<b>1.5 g WTR– Model Ver4</b>	143.35	0.001	0.72	15
<b>1 g WTR– Model Ver1</b>	<u>22.77904</u>	<u>0.738001</u>	<u>1</u>	<u>22.8</u>
<b>1 g WTR– Model Ver2</b>	-0.15673	0.280367	0.7537	22.8
<b>1 g WTR– Model Ver3</b>	0.000613	0.374002	0.7537	22.8
<b>1 g WTR– Model Ver4</b>	0.005212	0.000617	0.7497	22.8

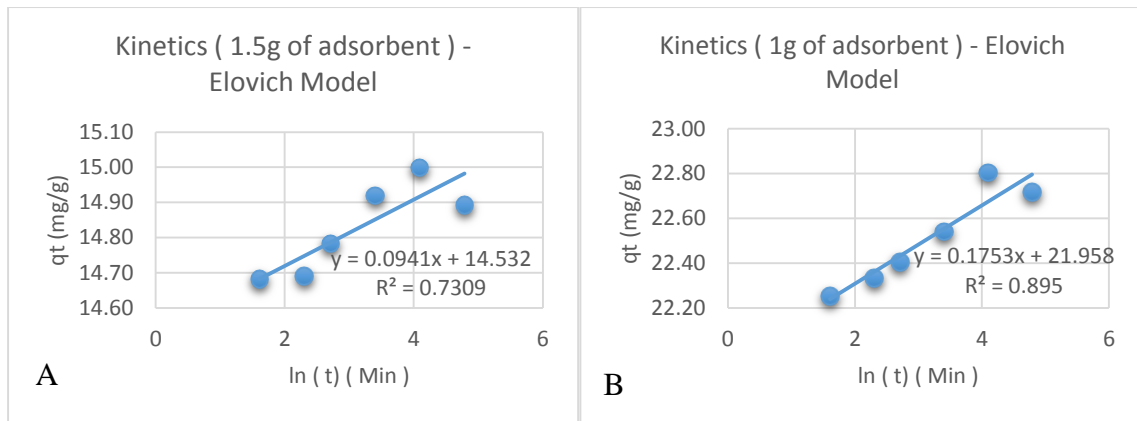


Figure 30 Elovich kinetic model fitted for adsorption study of WTR; where A: for 1.5g WTR, B: 1 g WTR ; Operational settings: Adsorbate mass : 1 g, Solution volume :1700 ml, Contact time : minutes, Temperature : 294.45 K , Rotation speed: 150 rpm , pH : 2.

Table 13 summarizes the final findings on using different kinetic models on the boron adsorption onto WTR. It shows that the pseudo-second order gives the best fit with an excellent linearity with a high correlation coefficient (100%). So, the pseudo-second order model was the best in describing the adsorption kinetics of boron onto both WTR dosages. In addition, the ARED value was 0.69 for 1 g WTR and 1.21 ARED for 1.5 g WTR; indicating the appropriateness of the model. The Elovich model also gave a relatively good fit linearity with medium to high correlation coefficient (0.73 and 0.90 for 1.5 g and 1 g WTR, respectively), and the ARED values were 28.31 ARED for 1 g and 74.5 ARED for 1.5 g WTR. In the pseudo-first order model, the experimental adsorption capacity did not equal the calculated adsorption capacity; therefore, the model does not fit the experimental data of the boron adsorption using WTR. In contrast, the pseudo-second order model agreed well in describing the adsorption kinetics of boron onto both WTR dosages. The agreement of the pseudo-second order model with the experimental data could be explained based on the assumption that the rate limiting step, as chemical sorption or chemisorption involving valency forces through sharing or exchange of electrons between adsorbent and adsorbate.

The adsorption system obeys the pseudo-second order model for the entire adsorption period and; thus supports the assumption behind the model that the adsorption is due to chemisorption. The adsorption of boron onto WTR surface takes place probably via surface exchange reactions until the surface functional sites are fully occupied (Bakar et al., 2016)

The general explanation for this form of kinetic law involves a variation of the energetics of chemisorption with the active sites that are heterogeneous WTR and therefore, exhibited different activation energies for chemisorption. Elovich model gives a good correlation for adsorption on highly heterogeneous surfaces and also it shows that the surface adsorption chemisorption was also a dominant phenomenon taking place. But, in a highly heterogeneous system, along with surface adsorption, chemisorption, ion exchange, precipitation and intra-particle diffusion may occur concurrently. In the case of using the Elovich equation, the correlation coefficients are lower than those of the pseudo-second order model (Bakar et al., 2016).

Table 15 presents the adsorption capacities of boron adsorption onto various Adsorbents. It can be observed that the boron adsorption capacity of this current study is showing the highest adsorption capacity comparing to the other investigators. This could be attributed to the pH value that was used in our study. in this study the pH was 4, but in their experiments the pH values were in mid-range of pH 5-9, thus knowing the unique characteristics of boron speciation by pH, could explain the difference (Schott et al., 2014).



Table 14: Adsorption Isotherms Of Boron For Various Adsorbents (Morisada Et Al., 2011)

<b>Adsorbent</b>	<b>qe [mg/g] at C<sub>0</sub>: 0.5 mg/l</b>	<b>Ref</b>
<b>TG</b>	2.48 x10 <sup>-2</sup>	(Morisada, Rinet al, 2011)
<b>ATG</b>	3.43 x10 <sup>-2</sup>	(Morisada, Rin, et al,2011)
<b>Polyol-grafted SBA-15</b>	2.61 x10 <sup>-1</sup>	(Wang, Qi, & Zhang, 2006)
<b>Polyol-grafted MCM-41</b>	6.11 x10 <sup>-2</sup>	(Wang et al., 2006)
<b>Activated carbon (AC)</b>	1.37 x10 <sup>-2</sup>	(Kluczka, 2015)
<b>AC with tartaric acid</b>	2.5 x10 <sup>-2</sup>	(Kluczka, 2015)
<b>AC with tartaric acid</b>	2.8 x10 <sup>-2</sup>	(Kluczka, 2015)
<b>Activated alumina</b>	1.17 x10 <sup>-2</sup>	(Kluczka, 2015)
<b>Zirconium dioxide</b>	2.78 x10 <sup>-2</sup>	(Kluczka, 2015)
<b>Cerium dioxide</b>	1.32 x10 <sup>-5</sup>	(Öztürk & Kavak, 2005)
<b>Calcined alunite</b>	1.93 x10 <sup>-2</sup>	(Kavak, 2009)
<b>Palm oil mill boiler bottom ash</b>	2.44 x10 <sup>-5</sup>	Chong et al., 2009
<b>WTR</b>	1.3 [Freundlich model]	This study
<b>Chemically Modified-WTR</b>	1.69 [Freundlich model]	This study
<b>Nano-WTR</b>	0.74 [Freundlich model]	This study

## Chapter 5: Conclusion

In this study, the boron adsorption was investigated using WTR, chemically modified-WTR and nano-WTR. Different key parameters such as initial boron concentration, adsorbent mass, particle size, pH, and contact time were thoroughly investigated. Accordingly, the following conclusions can be drawn from the study:

- The boron adsorption onto the WTR was affected by the key adsorption parameters such as adsorbent dosage, initial concentration, particle size, contact time and pH.
- For the pH, the highest adsorption capacity was at pH 2 at the value of  $8.45 \pm 0.01$  mg/g.
- It was observed that an increase in adsorbent dosage was followed by a decrease in boron adsorption capacity; signifying that the adsorption process was dramatically influenced by the adsorbent dose. The highest adsorption capacity was at dosage of 0.05 g WTR at the value of  $5.322 \pm 0.005$  mg/g. The result can be explained due to most of the boron was already adsorbed when the dosage was high; therefore, as the dosage increase, the initial boron concentration goes down rapidly and cannot keep up with available sites to bind to. The solution would be to increase the initial boron concentration to 200 mg/L instead of 50 mg/L.
- The kinetic adsorption was rapid and achieved within 65 minutes.
- The boron adsorption capacity was decreased when the particle size increased. The highest boron adsorption capacity was recorded at  $8.32 \pm 0.00$  mg/g for WTR particle size in the range of 125-1000  $\mu\text{m}$ .
- The highest adsorption capacities for Boron was observed in chemically modified-WTR, followed by WTR and followed by Nano-WTR.
- It was concluded that the Freundlich isotherm and pseudo second order kinetic models were well fitted to the isotherm and kinetic experimental data, respectively.

- This study confirms that the WTR can be widely used for removal of boron from aqueous solution at a cost-efficient adsorbent. Furthermore, it can be observed that the boron adsorption capacity of this current study was showing the highest adsorption capacity comparing to the other investigators.
- The highest Leachability was for Zn in the amount of 1635  $\mu\text{g/L}$  from WTR. This trend is quite logical since the Zn make up almost 2 % weight of WTR according to Elemental analysis using EDX. The trend was followed by Fe (179.45  $\mu\text{g/L}$ ), Pb (117.41  $\mu\text{g/L}$ ), Cd (6.83  $\mu\text{g/L}$ ) and Cr 0.44  $\mu\text{g/L}$ ). It also observed decrease in pH lead to increase Zn, Pb and Fe Leachability.
- It is recommended to have further investigations on other key parameters such as rotation speed, temperature, flow rate and pressure in order to apply the adsorbent in industrial scale.
- It is recommended to investigate the porosity and surface area and other surface characteristics of WT adsorbent is advised to fully understand the adsorption process, and shed light on the behavior of particle size in the study.
- It also recommended to apply particle size analysis for micro and Nano size particles of WT, to ensure the uniformity of size category.
- It also recommended to use more sophisticated kinetics models and isotherms models , to get better representation on mechanism of adsorption
- It is highly recommended to investigate the applicability of using spent WTR adsorbent, as it is one of the key criteria of choosing good adsorbents.
- Finally, further investigation of WT capacity to adsorb mixture of pollutants is recommended.

## References

- Ahmaruzzaman, M. (2008). Adsorption of phenolic compounds on low-cost adsorbents: A review. *Advances in Colloid and Interface Science*. <https://doi.org/10.1016/j.cis.2008.07.002>
- Aisien, F. ., Amenaghawon, N. ., & Agho, O. E. (2013). Application of Recycled Rubber from Scrap Tire in the Removal of Toluene from Aqueous Solution. *The Pacific Journal of Science and Technology*, 14(2), 230–241. Retrieved from [http://www.researchgate.net/profile/Andrew\\_Amenaghawon/publication/259214254\\_Application\\_of\\_Recycled\\_Rubber\\_from\\_Scrap\\_Tire\\_in\\_the\\_Removal\\_of\\_Phenol\\_from\\_Aqueous\\_Solution/links/0046352a70b4a7d824000000.pdf](http://www.researchgate.net/profile/Andrew_Amenaghawon/publication/259214254_Application_of_Recycled_Rubber_from_Scrap_Tire_in_the_Removal_of_Phenol_from_Aqueous_Solution/links/0046352a70b4a7d824000000.pdf)
- Aisien, F. A., Amenaghawon, N. A., & Akhidenor, S. A. (2013). Adsorption of Ethylbenzene from Aqueous Solution Using Recycled Rubber from Scrap Tyre. *Journal of Scientific Research & Reports*, 2(2), 497–512.
- Al-Ghouti, M. A., Khraisheh, M. A. M., Allen, S. J., & Ahmad, M. N. (2003). The removal of dyes from textile wastewater: A study of the physical characteristics and adsorption mechanisms of diatomaceous earth. *Journal of Environmental Management*, 69(3), 229–238. <https://doi.org/10.1016/j.jenvman.2003.09.005>
- Alam, M. J. B., Dikshit, A. K., Banerjee, M., Reza, I., & Rahman, A. M. (2006). Study of Sorption of 2,4- D on Outer Peristaltic Part of Waste Tire Rubber Granules. *Journal of Dispersion Science and Technology*, 27(6), 843–849. <https://doi.org/10.1080/01932690600719115>
- Allen, S. J., McKay, G., & Porter, J. F. (2004). Adsorption isotherm models for basic dye adsorption by peat in single and binary component systems. *Journal of Colloid and Interface Science*, 280(2), 322–333. <https://doi.org/10.1016/j.jcis.2004.08.078>

- Amrita institute of education. (2012). Adsorption Isotherm Objective & Theory. Retrieved from <http://vlab.amrita.edu/?brch=190&cnt=1&sim=606&sub=2>
- ASTOM. (2013). Ion exchange membrane [NEOSEPTA].
- Ayyildiz, H. F., & Kara, H. (2005). Boron removal by ion exchange membranes. *Desalination*, *180*(1–3), 99–108. <https://doi.org/10.1016/j.desal.2004.12.031>
- Bakar, A. H. B. A., Koay, Y. S., Ching, Y. C., Abdullah, L. C., Choong, T. S. Y., Alkhatib, M., ... Zahri, N. A. M. (2016). Removal of fluoride using quaternized palm kernel shell as adsorbents: Equilibrium isotherms and kinetics studies. *BioResources*, *11*(2), 4485–4511. <https://doi.org/10.15376/biores.11.2.4485-4511>
- Blevins, D. G., & Lukaszewski, K. M. (1998). BORON IN PLANT STRUCTURE AND FUNCTION, 481–500.
- Chan, L. S., Cheung, W. H., Allen, S. J., & McKay, G. (2012). Error analysis of adsorption isotherm models for acid dyes onto bamboo derived activated carbon. *Chinese Journal of Chemical Engineering*, *20*(3), 535–542. [https://doi.org/10.1016/S1004-9541\(11\)60216-4](https://doi.org/10.1016/S1004-9541(11)60216-4)
- Christmann, K. (2012). Thermodynamics and Kinetics of Adsorption. *Institut Für Chemie Und Biochemie, Freie Universität Berlin*. Retrieved from [http://w0.rz-berlin.mpg.de/imprs-cs/download/Vortrag\\_IMPRS\\_Schmoeckwitz\\_Mi\\_9-11\\_KChrist.pdf](http://w0.rz-berlin.mpg.de/imprs-cs/download/Vortrag_IMPRS_Schmoeckwitz_Mi_9-11_KChrist.pdf)
- Colom, X., Faliq, A., Formela, K., & Caavate, J. (2016). FTIR spectroscopic and thermogravimetric characterization of ground tyre rubber devulcanized by microwave treatment. *Polymer Testing*, *52*, 200–208. <https://doi.org/10.1016/j.polymertesting.2016.04.020>
- Cunliffe, A. M., & Williams, P. T. (1998). Composition of oils derived from the batch pyrolysis of tyres. *Journal of Analytical and Applied Pyrolysis*, *44*(2), 131–152.

[https://doi.org/10.1016/S0165-2370\(97\)00085-5](https://doi.org/10.1016/S0165-2370(97)00085-5)

- Datta, J., & Wloch, M. (2015). Morphology and properties of recycled polyethylene/ground tyre rubber/thermoplastic poly(ester-urethane) blends. *Macromolecular Research*, 23(12), 1117–1125. <https://doi.org/10.1007/s13233-015-3155-5>
- El-Sherif, I. Y., Farah, J. Y., Girgis, E., & Mohamed, O. A. (2013). Removal of chromium from tannery wastewater using magnetic nanoparticles. *Journal of Applied Sciences Research*, 9(3), 1564–1572. <https://doi.org/10.1067/mmt.2002.123333>
- Engates, K. E., & Shipley, H. J. (2011). Adsorption of Pb, Cd, Cu, Zn, and Ni to titanium dioxide nanoparticles: Effect of particle size, solid concentration, and exhaustion. *Environmental Science and Pollution Research*, 18(3), 386–395. <https://doi.org/10.1007/s11356-010-0382-3>
- EPRI. (2007). *Treatment Technology Summary for Critical Pollutants of Concern in Power Plant Wastewaters*.
- Farouq, R., & Yousef, N. S. (2014). Equilibrium and Kinetics Studies of adsorption of Copper (II) Ions on Natural Biosorbent. *International Journal of Chemical Engineering and Applications*, 11(5), 61. <https://doi.org/10.7763/IJCEA.2015.V6.503>
- Farzaneh Jahanbakhsh, B. E. (2016). Modified Activated Carbon with Zinc Oxide Nanoparticles Produced from Used Tire for Removal of Acid Green 25 from Aqueous Solutions. *American Journal of Applied Chemistry*, 4(1), 8–13. <https://doi.org/10.11648/j.ajac.20160401.12>
- Foo, K. Y., & Hameed, B. H. (2010). Insights into the modeling of adsorption isotherm systems. *Chemical Engineering Journal*. <https://doi.org/10.1016/j.cej.2009.09.013>
- Garg, U., Kaur, M. P., Jawa, G. K., Sud, D., & Garg, V. K. (2008). Removal of cadmium (II) from aqueous solutions by adsorption on agricultural waste biomass. *Journal of Hazardous Materials*, 154(1–3), 1149–1157.

<https://doi.org/10.1016/j.jhazmat.2007.11.040>

- Ghasemi, N., Tamri, P., Khademi, A., Nezhad, N. S., & Alwi, S. R. W. (2013). Linearized Equations of Pseudo Second-order Kinetic for the Adsorption of Pb(II) on Pistacia Atlantica Shells. *IERI Procedia*, 5, 232–237. <https://doi.org/10.1016/j.ieri.2013.11.097>
- Ghosh, P., Katare, S., Patkar, P., Caruthers, J. M., Venkatasubramanian, V., & Walker, K. A. (2003). Sulfur Vulcanization of Natural Rubber for Benzothiazole Accelerated Formulations: From Reaction Mechanisms to a Rational Kinetic Model. *Rubber Chemistry and Technology*, 76(3), 592–693. <https://doi.org/10.5254/1.3547762>
- Gleadthorpe, A. (2008). heavy meatal input in England, 2007(February), 1–35.
- Gonzalez, J. F., Encinar, J. M., Canito, J. L., & Rodriguez, J. J. (2001). Pyrolysis of automobile tyre waste. Influence of operating variables and kinetics study. *Journal of Analytical and Applied Pyrolysis*, 58(59), 667–683. [https://doi.org/10.1016/S0165-2370\(00\)00201-1](https://doi.org/10.1016/S0165-2370(00)00201-1)
- Güler, E., Kaya, C., Kabay, N., & Arda, M. (2015). Boron removal from seawater: State-of-the-art review. *Desalination*, 356, 85–93. <https://doi.org/10.1016/j.desal.2014.10.009>
- Gunasekaran, S., Natarajan, R. K., & Kala, A. (2007). FTIR spectra and mechanical strength analysis of some selected rubber derivatives. *Spectrochimica Acta - Part A: Molecular and Biomolecular Spectroscopy*, 68(2), 323–330. <https://doi.org/10.1016/j.saa.2006.11.039>
- Guo, C., Zhou, L., & Lv, J. (2013). Effects of expandable graphite and modified ammonium polyphosphate on the flame-retardant and mechanical properties of wood flour-polypropylene composites. *Polymers and Polymer Composites*, 21(7), 449–456. <https://doi.org/10.1002/app>
- Gupta, S., & Babu, B. V. (2009). Removal of toxic metal Cr(VI) from aqueous solutions using sawdust as adsorbent: Equilibrium, kinetics and regeneration studies. *Chemical*

- Engineering Journal*, 150(2–3), 352–365. <https://doi.org/10.1016/j.cej.2009.01.013>
- Haghseresht, F., & Lu, G. Q. (1998). Adsorption Characteristics of Phenolic Compounds onto Coal-Reject-Derived Adsorbents. *Energy & Fuels*, 12(6), 1100–1107. <https://doi.org/10.1021/ef9801165>
- Henning, K. D., & Degel, J. (1990). Activated carbon for solvent recovery. In *meeting of the European Rotogravure Association engineers group* (pp. 20–21).
- Imyim, A., Sirithaweessit, T., & Ruangpornvisuti, V. (2016). Arsenite and arsenate removal from wastewater using cationic polymer-modified waste tyre rubber. *Journal of Environmental Management*, 166, 574–578. <https://doi.org/10.1016/j.jenvman.2015.11.005>
- Karcher, S., Kornmüller, A., & Jekel, M. (2001). Screening of commercial sorbents for the removal of reactive dyes. *Dyes and Pigments*, 51(2–3), 111–125. [https://doi.org/10.1016/S0143-7208\(01\)00066-3](https://doi.org/10.1016/S0143-7208(01)00066-3)
- Karthikeyan, G., & Siva Ilango, S. (2008). Equilibrium Sorption studies of Fe , Cu and Co ions in aqueous medium using activated Carbon prepared from *Recinius Communis Linn* . *Journal of Applied Science and Environment Management*, 12(2), 81–87.
- Kavak, D. (2009). Removal of boron from aqueous solutions by batch adsorption on calcined alunite using experimental design. *Journal of Hazardous Materials*, 163(1), 308–314. <https://doi.org/10.1016/j.jhazmat.2008.06.093>
- Kim, B. J. Y., Park, J. K., & Edil, T. B. (1997). Sorption of Organic Compounds in the Aqueous Phase I }.
- Kluczka, J. (2015). Boron removal from fqueous solutions using an fmorphous zirconium dioxide. *Int. J. Environ. Res.*, 9(2), 711–720.
- Krishna, R. H., & Swamy, A. V. V. S. (2012). Investigation On The Effect Of Particle Size And Adsorption Kinetics For The Removal Of Cr (Vi ) From The Aqueous Solutions



- Using Low Cost Sorbent. *Eur. Chem. Bull.*, (Vi), 258–262.
- Lee, J., Lee, J., Kim, J., & Kim, S. D. (1995). PYROLYSIS OF WASTE TIRES WITH PARTIAL OXIDATION IN A FLUIDIZED-BED REACTOR. *Energy*, :969-976.
- Li, P., Liu, C., Zhang, L., Zheng, S., & Zhang, Y. (2017). Enhanced boron adsorption onto synthesized MgO nanosheets by ultrasonic method. *Ultrasonics Sonochemistry*, 34, 938–946. <https://doi.org/10.1016/j.ultsonch.2016.07.029>
- Manchon Vizuete, E., Macias Garcia, A., Gisbert, A. N., Ferniandez Gonzialez, C., & Gomez-Serrano, V. (2004). Preparation of mesoporous and macroporous materials from rubber of tyre wastes. *Microporous and Mesoporous Materials*, 67(1), 35–41. <https://doi.org/10.1016/j.micromeso.2003.10.002>
- Mazille, F., & Spuhler, D. (2012). Membrane Filtration. <https://doi.org/10.1002/9781118131473>
- MDPS. (2015). *Qatar Economic Outlook 2016–2018*. Doha. Retrieved from [http://www.mdps.gov.qa/en/knowledge/Doc/QEO/Qatar\\_Economic\\_Outlook\\_2016\\_2018\\_EN.pdf](http://www.mdps.gov.qa/en/knowledge/Doc/QEO/Qatar_Economic_Outlook_2016_2018_EN.pdf)
- Mittal, A., Mittal, J., Malviya, A., & Gupta, V. K. (2010). Removal and recovery of Chrysoidine Y from aqueous solutions by waste materials. *Journal of Colloid and Interface Science*, 344(2), 497–507. <https://doi.org/10.1016/j.jcis.2010.01.007>
- Moghaddasi, S., Khoshgoftarmanesh, A. H., Karimzadeh, F., & Chaney, R. L. (2013). Preparation of nano-particles from waste tire rubber and evaluation of their effectiveness as zinc source for cucumber in nutrient solution culture. *Scientia Horticulturae*, 160, 398–403. <https://doi.org/10.1016/j.scienta.2013.06.028>
- Morisada, S., Rin, T., Ogata, T., Kim, Y. H., & Nakano, Y. (2011). Adsorption removal of boron in aqueous solutions by amine-modified tannin gel. *Water Research*, 45(13), 4028–4034. <https://doi.org/10.1016/j.watres.2011.05.010>

- Mousavi, H. Z., Hosseynifar, A., Jahed, V., & Dehghani, S. A. M. (2010). Removal of lead from aqueous solution using waste tire rubber ash as. *Brazilian Journal of Chemical Engineering*, 27(1), 79–87. <https://doi.org/10.1590/S0104-66322010000100007>
- Namasivayam, C., & Kavitha, D. (2002). Removal of Congo Red from water by adsorption onto activated carbon prepared from coir pith, an agricultural solid waste. *Dyes and Pigments*, 54(1), 47–58. [https://doi.org/10.1016/S0143-7208\(02\)00025-6](https://doi.org/10.1016/S0143-7208(02)00025-6)
- Nieto-márquez, A., Pinedo-flores, A., Picasso, G., & Atanes, E. (2017). Journal of Environmental Chemical Engineering Selective adsorption of Pb 2 + , Cr 3 + and Cd 2 + mixtures on activated carbons prepared from waste tires, 5, 1060–1067. <https://doi.org/10.1016/j.jece.2017.01.034>
- Öztürk, N., & Kavak, D. (2005). Adsorption of boron from aqueous solutions using fly ash: Batch and column studies. *Journal of Hazardous Materials*, 127(1–3), 81–88. <https://doi.org/10.1016/j.jhazmat.2005.06.026>
- Park, J. K., Bontoux, L., Holsen, T. M., Jenkins, D., & Selleck, R. E. (1991). Permeation of polybutylene pipe and gasket material by organic chemicals. *Journal / American Water Works Association*, 83(10), 71–78.
- Parks, J. L., & Edwards, M. (2005). Boron in the Environment. *Critical Reviews in Environmental Science and Technology*, 35(2), 81–114. <https://doi.org/10.1080/10643380590900200>
- Prats, D., Chillón-Arias, M. F., & Rodríguez-Pastor, M. (2000). Analysis of the influence of pH and pressure on the elimination of boron in reverse osmosis. *Desalination*, 128(3), 269–273. [https://doi.org/10.1016/S0011-9164\(00\)00041-2](https://doi.org/10.1016/S0011-9164(00)00041-2)
- Redondo, J., Busch, M., & De Witte, J. P. (2003). Boron removal from seawater using FILMTEC high rejection SWRO membranes. *Desalination*, 156(1–3), 229–238. [https://doi.org/10.1016/S0011-9164\(03\)00345-X](https://doi.org/10.1016/S0011-9164(03)00345-X)

- Riahi, K., Chaabane, S., & Thayer, B. Ben. (2013). A kinetic modeling study of phosphate adsorption onto Phoenix dactylifera L. date palm fibers in batch mode. *Journal of Saudi Chemical Society*. <https://doi.org/10.1016/j.jscs.2013.11.007>
- Rungrodnimitchai, S., & Kotatha, D. (2015a). Chemically Modification of Ground Tire Rubber. *Chemical Engineering Journal*, 282, 161–169.
- Rungrodnimitchai, S., & Kotatha, D. (2015b). Chemically modified ground tire rubber as fluoride ions adsorbents. *Chemical Engineering Journal*, 282, 161–169. <https://doi.org/10.1016/j.cej.2015.03.038>
- Sagle, A., & Freeman, B. (2004). Fundamentals of membranes for water treatment. *The Future of Desalination in Texas*, (The future of desalination in Texas), 1–17. Retrieved from [http://www.twdb.state.tx.us/publications/reports/numbered\\_reports/doc/R363/C6.pdf](http://www.twdb.state.tx.us/publications/reports/numbered_reports/doc/R363/C6.pdf)
- Schott, J., Kretzschmar, J., Acker, M., Eidner, S., Kumke, M. U., Drobot, B. B., ... Stumpf, T. (2014). Formation of a Eu(III) borate solid species from a weak Eu(III) borate complex in aqueous solution. *Dalton Transactions (Cambridge, England : 2003)*, 43(30), 11516–11528. <https://doi.org/10.1039/c4dt00843j> PM - 24849080 M4 - Citavi
- Shimazu Corporation. (2016). *Analysis of Black Rubber Diaphragm by FTIR and EDX*.
- Sivaraj, R., Namasivayam, C., & Kadirvelu, K. (2001). Orange peel as an adsorbent in the removal of Acid violet 17 (acid dye) from aqueous solutions. *Waste Management*, 21(1), 105–110. [https://doi.org/10.1016/S0956-053X\(00\)00076-3](https://doi.org/10.1016/S0956-053X(00)00076-3)
- Smith, C. C., Anderson, W. F., & Freewood, R. J. (2001). Evaluation of shredded tyre chips as sorption media for passive treatment walls. *Engineering Geology*, 60(1–4), 253–261. [https://doi.org/10.1016/S0013-7952\(00\)00106-X](https://doi.org/10.1016/S0013-7952(00)00106-X)
- Strathmann, H. (2004). Ion-exchange membrane separation processes. In *Ion-exchange membrane separation processes*. Elsevier. <https://doi.org/10.1002/14356007.a16>

- Taimur, K., & Malay, C. (2011). Adsorption capacity of coconut coir activated carbon in the removal of disperse and direct dyes from aqueous solution. *Research Journal of Chemistry and Environment*, 15(2), 601–605.
- Tutu, H., Bakatula, E., Dlamini, S., Rosenberg, E., Kailasam, V., & Cukrowska, E. M. (2013). Kinetic, equilibrium and thermodynamic modelling of the sorption of metals from aqueous solution by a silica polyamine composite. *Water SA*, 39(4), 437–444.
- US-EPA. (2014). Drinking Water Treatability Database. Retrieved from <https://iaspub.epa.gov/tdb/pages/general/home.do>
- Wang, L., Qi, T., & Zhang, Y. (2006). Novel organic-inorganic hybrid mesoporous materials for boron adsorption. *Colloids and Surfaces A: Physicochemical and Engineering Aspects*, 275(1–3), 73–78. <https://doi.org/10.1016/j.colsurfa.2005.06.075>
- WaterTectonics. (2017). What is Electrocoagulation (EC)? *Electrocoagulation*. WaterTectonics.
- Weber, W. J., McGinley, P. M., & Katz, L. E. (1991). Sorption phenomena in subsurface systems: Concepts, models and effects on contaminant fate and transport. *Water Research*, 25(5), 499–528. [https://doi.org/10.1016/0043-1354\(91\)90125-A](https://doi.org/10.1016/0043-1354(91)90125-A)
- Xu, Y., & Jiang, J. Q. (2008). Technologies for boron removal. *Industrial and Engineering Chemistry Research*, 47(1), 16–24. <https://doi.org/10.1021/ie0708982>
- Yüksel, S., & Yürüm, Y. (2009). Removal of Boron from Aqueous Solutions by Adsorption Using Fly Ash, Zeolite, and Demineralized Lignite. *Separation Science and Technology*, 45(1), 105–115. <https://doi.org/10.1080/01496390903256042>
- Yun, Y. K. (2008). Division of Environmental Science and Engineering Division of Environmental Science and Engineering EG2605 UROP Report Methylene blue adsorption by pyrolytic tyre char, 1–10.
- Zalloum, H. M., Al-Qodah, Z., & Mubarak, M. S. (2008). Copper Adsorption on Chitosan-

Derived Schiff Bases. *Journal of Macromolecular Science, Part A*, 46(1), 46–57.

<https://doi.org/10.1080/10601320802515225>